



**HAL**  
open science

## Environmental changes and the rise and fall of civilizations in the northern Horn of Africa: an approach combining $\delta D$ analyses of land-plant derived fatty acids with multiple proxies in soil

Valery T. Terwilliger, Zewdu Eshetu, Jean-Robert Disnar, Jérémy Jacob, Paul W. Adderley, Yongsong Huang, Marcelo Alexandre, Marylin L. Fogel

### ► To cite this version:

Valery T. Terwilliger, Zewdu Eshetu, Jean-Robert Disnar, Jérémy Jacob, Paul W. Adderley, et al.. Environmental changes and the rise and fall of civilizations in the northern Horn of Africa: an approach combining  $\delta D$  analyses of land-plant derived fatty acids with multiple proxies in soil. *Geochimica et Cosmochimica Acta*, 2013, 111, pp.140-161. 10.1016/j.gca.2012.10.040 . insu-00749909

**HAL Id: insu-00749909**

**<https://insu.hal.science/insu-00749909>**

Submitted on 12 Nov 2012

**HAL** is a multi-disciplinary open access archive for the deposit and dissemination of scientific research documents, whether they are published or not. The documents may come from teaching and research institutions in France or abroad, or from public or private research centers.

L'archive ouverte pluridisciplinaire **HAL**, est destinée au dépôt et à la diffusion de documents scientifiques de niveau recherche, publiés ou non, émanant des établissements d'enseignement et de recherche français ou étrangers, des laboratoires publics ou privés.

Environmental changes and the rise and fall of civilizations in the northern Horn of Africa: an approach combining  $\delta D$  analyses of land-plant derived fatty acids with multiple proxies in soil.

Valery J. Terwilliger<sup>a,b,c,\*</sup>, Zewdu Eshetu<sup>d</sup>, Jean-Robert Disnar<sup>b</sup>, Jérémy Jacob<sup>b</sup>, W. Paul Adderley<sup>e</sup>, Yongsong Huang<sup>f</sup>, Marcelo Alexandre<sup>g</sup>, Marilyn L. Fogel<sup>h</sup>

<sup>a</sup> University of Kansas, Department of Geography, Lawrence, KS, USA

<sup>b</sup> Institut des Sciences de la Terre d'Orléans (ISTO), Université d'Orléans, UMR 7327 du CNRS/INSU, Orléans, France

<sup>c</sup> LE STUDIUM®, Loire Valley Institute for Advanced Studies, Orléans, France

<sup>d</sup> University of Addis Ababa, Department of Paleoanthropology and Paleoenvironment, Addis Ababa, Ethiopia

<sup>e</sup> University of Stirling, Biological and Environmental Sciences, School of Natural Sciences, Stirling, Scotland, UK

<sup>f</sup> Brown University, Department of Geological Sciences, Providence, RI, USA

<sup>g</sup> Universidade Federal de Sergipe, Departamento de Química, São Cristóvão, Brasil

<sup>h</sup> Carnegie Institution of Washington, Geophysical Laboratory, Washington, DC, USA

\* Corresponding author. Tel.: +1 785 864 5143  
E-mail address: [terwilli@ku.edu](mailto:terwilli@ku.edu)

Submit to: *Geochimica et Cosmochimica Acta*

Key words: stable isotopes,  $\delta D$  *n*-alkanoic acids, soil image-analysis, Rock-eval pyrolysis, paleoenvironmental reconstruction, soil organic matter, Ethiopian Plateau

## 1 **Abstract**

2 The domains of the ancient polities D'MT and Aksum in the Horn of Africa's highlands are a  
3 superior natural system for evaluating roles of environmental change on the rise and fall of  
4 civilizations. To compare environmental changes of the times of the two polities, we  
5 analyzed stable hydrogen isotopic ratios ( $\delta D$ ) of land-plant derived fatty acids ( $n\text{-C}_{26-30}$ ) and  
6 other proxies from soil sequences spanning the Holocene from the region. Three results  
7 suggest that trends in  $\delta D$  values unambiguously reflect changes in rainfall. First, increases in  
8  $\delta D$  coincide with dry periods inferred from studies of eastern African lakes. Second, changes  
9 in  $\delta D$  values were parallel among sections during overlapping time intervals. Third,  
10 consideration of vegetation history did not alter directions of trends in  $\delta D$  values over time.  
11 By unambiguously recording precipitation, the  $\delta D$  values also enhanced interpretations of  
12 proxies that are affected by both climate and land clearing.

13 Both D'MT (ca 2750–2350 cal y BP) and the Aksumite (ca 2100–1250 cal y BP) rose  
14 during wetter intervals of the drier part of the Holocene (after ca 6000 cal y BP). Analyses of  
15 charred matter indicated that fire had been a common agent of land clearing in all sites. The  
16 influence of climate on fire varied, however. Prior to the emergence of D'MT,  $\delta D$  values were  
17 correlated with  $C_4:C_3$  plant ratios estimated from  $\delta^{13}C$  values. There are no  $C_4$  trees and  
18 precipitation may have been the main influence on canopy openness. After ca 4300 cal y  
19 BP, there was no significant relationship between  $\delta D$  and  $C_4:C_3$  plant ratios suggesting that  
20 factors such as fire influenced canopy openness regardless of climate. Furthermore, the  
21 impact of land clearance differed between sites and between D'MT and the Aksumite's times.  
22 In one site, the interval from 3550 cal y BP to the decline of D'MT had several anomalies that  
23 suggested dramatic increases in thermal severity of fire and human impact. Among these  
24 were a large contribution of charred matter to a high % total organic carbon that low  
25 hydrogen and oxygen indices suggest was severely altered by other factors than  
26 humification. These results support hypotheses about the rise of civilizations being favored  
27 by specific climatic conditions but suggest that patterns of land clearing differed during the  
28 declines of D'MT and the Aksumite.

## 29 1. INTRODUCTION

30 Environmental changes have been linked to as widely ranging factors shaping the  
31 complexity of civilizations as food security and attitudes about non-conformity (Diamond,  
32 2005; Büntgen et al., 2011; Gelfand et al., 2011). Research to understand the nature of links  
33 between past environments and the rise and fall of civilizations is sought for managing  
34 consequences of present global environmental changes (CCSP, 2003; IPCC, 2007;  
35 Mastrandea and Schneider, 2010). Paleoenvironmental records have been a key  
36 component of such research (Aimers, 2011).

37 Needs for progress are now recognized in two applications of paleoenvironmental  
38 records to evaluate effects of environment on cultural complexity. One need is better local-  
39 scale environmental records (Dergachev et al., 2007; Emery and Thornton, 2008; Giorgi et  
40 al., 2008; Jones et al., 2009; Hodell, 2011). This is a prerequisite to the larger need to  
41 understand if certain environmental changes have predictable consequences for the status of  
42 civilizations (Turchin, 2008; Beck et al., 2010). Consequences of environmental changes for  
43 civilizations have largely been deduced by linking climate records to land clearing  
44 characteristics and then to historical developments in a single polity (e.g. McGovern, 1994;  
45 deMenocal, 2001; Weiss and Bradley, 2001; Haug et al., 2003; Adderley and Simpson, 2006;  
46 Patterson et al., 2010). A strategy to understand whether environmental changes have  
47 predictable consequences for civilizations is to study locations where more than one complex  
48 polity has risen and fallen (Gebru et al., 2009; Terwilliger et al., 2011).

49 The Tigray Plateau of the northern Horn of Africa (hereinafter called the Plateau) has  
50 prime attributes for contributing to both of the aforementioned needs. Mountainous relief,  
51 location along the northern oscillations of the Inter-Tropical Convergence Zone, and  
52 proximity to an active triple junction of plate tectonic activity assure large spatial and  
53 temporal changes in environment. The Plateau's networks of gullies expose soil sequences  
54 that have rich archives of proxies for local-scale environmental changes during continuous  
55 time intervals throughout the Holocene (Berakhi et al., 1998; Machado, 1998; Dramis et al.,  
56 2003; Gebru et al., 2009; Terwilliger et al., 2011). The succession of complex polities that

57 existed there during the Holocene make the Plateau a superior natural laboratory for  
58 examining whether environment predictably affects the status of societies. Among these was  
59 one of the major ancient civilizations of the world -- the Aksumite Empire (Duiker and  
60 Spielvogel, 2010). D'MT, which preceded Aksum, had a similar suite of the accoutrements of  
61 a civilization (Fattovich 1990, 2000, 2009; Robin and de Maigret, 1998; Bard et al., 2000).

62         Regardless of its importance, few studies of environmental history have been carried  
63 out on the Plateau (French, 2009; Sulas, 2010). Although likely including environmental  
64 effects, the reasons for the rise and fall of the Aksumite Empire are the least known of the  
65 major ancient civilizations (Butzer, 1981; Ehret, 2002; Connah, 2004). Whether  
66 environmental factors played similar roles on the emergence and disintegration of both D'MT  
67 and Aksum is unknown. The few paleoenvironmental records of the Plateau are largely  
68 derived from classical analyses of soil geomorphology. Conclusions about precipitation and  
69 land clearing patterns vary markedly among these studies (reviewed in Nyssen et al., 2004).  
70 Because precipitation or land clearing may have similar impacts on physical landscapes,  
71 these differences in interpretation may be irreconcilable using those methods alone (Butzer,  
72 2005).

73         Records from an unambiguous proxy for precipitation can be used to more clearly  
74 interpret proxies affected by climate and land clearing (Gebru et al., 2009; Terwilliger et al.,  
75 2008, 2011). Stable hydrogen isotopic analyses of land-plant derived lipid compounds  
76 extracted from soils and aquatic sediments are promising sources of information about  
77 paleohydrology (Sachse et al., 2012). The original source of hydrogen for lipid synthesis is  
78 water used in photosynthesis and the basis for the climate signal in the lipid is the influence  
79 of climate on the  $\delta D$  of that water (Dansgaard, 1964; Sternberg, 1989). Exactly how variable  
80 that influence is among plant types and how constant the hydrogen fractionation is from  
81 source water to specific lipid synthesis remain active areas of research, however, with  
82 implications meriting consideration in paleoclimate interpretation (e.g., Sachse et al., 2004,  
83 2006; Hou et al., 2008; Feakins and Sessions, 2010a; Garcin et al., 2012).

84         The main objective of this paper is to examine whether environments within the two

85 most complex of the Plateau's ancient polities; D'MT (ca 2750–2350 cal y BP) and the  
86 Aksumite Empire (ca 2100–1250 cal y BP), were similar at similar stages of development.  
87 This is a contribution to addressing the question “do certain environmental changes have  
88 predictable consequences for the rise and fall of civilizations?” For this purpose, we built  
89 records of local-scale climate and land clearing changes from proxies in exposed soil  
90 sequences at several sites that were within the domains of both D'MT and Aksum. These  
91 include analyses of  $\delta D$  values of land-plant derived saturated fatty acid compounds,  $\delta^{13}C$  of  
92 bulk organic matter, fire-related soil micro-imagery, elements (of P and organic C), and  
93 organic matter quality (Rock-Eval pyrolysis). This study is distinctive in its use of  
94 paleoprecipitation records from molecular level  $\delta D$  analyses to reduce ambiguities in  
95 inferences about land clearing from other proxies.

96

## 97 **2. SAMPLING SITES AND STRATEGY**

### 98 **2.1. Site locations, environments, and history**

99 The Plateau was the site of a long, rich history of human groups that were at least as  
100 complex as kingdoms. Indications are that D'MT and Aksum were the most complex of  
101 these, attaining the accoutrements associated with many definitions of a civilization. These  
102 included novel writing systems, an urban center, international trade, agricultural innovation,  
103 a hinterland of agricultural communities, metallurgy, plow agriculture, water management  
104 technologies, and monumental stone architecture (DiBlasi, 2005; Fattovich, 2009). This  
105 paper particularly concerns itself with the environments during the times of the rise and fall of  
106 D'MT (ca 2750–2350 cal y BP) and of Aksum (ca 2100–1250 cal y BP) but see Gebru et al.  
107 (2009) for a more comprehensive summary timeline of developments in major polities of the  
108 Plateau .

109 We selected three sites with gullies exposing soil profiles in an Ethiopian portion of  
110 the Plateau that was first in D'MT and later in the Aksumite Empire (Fig. 1). We use the word  
111 “soil” in this paper to refer to unconsolidated deposits that are not under water, regardless of  
112 whether horizon development has occurred. Sites were chosen in the hinterlands of the

113 civilizations. Named after their nearest towns, they are Adi Kolan (AK, 2171 m a. s. l.), Mai  
114 Maikden (MM, 2228 m a. s. l.), and Adigrat (AT, 2493 m a. s. l.). Although none is a known  
115 archeological settlement site, their physical characteristics and proximity to known ancient  
116 settlements suggest long agricultural histories (Phillipson, 1998; D'Andrea et al., 2008; 2011;  
117 Curtis, 2009).

118         The sites have similar rainfall distributions but temperature decreases and rainfall  
119 increases slightly from the lowest (AK, 563 mm y<sup>-1</sup>) to the highest (AT, 619 mm y<sup>-1</sup>)  
120 elevations (National Meteorological Agency of Ethiopia, 1998–2006). The watersheds of all  
121 three sites have nearly identical plant cover consisting mostly of heavily grazed *Acacia* spp.  
122 dominated grassland and fit the description of floodplain as they are flat and surrounded by  
123 mountains (Fig. 1). This vegetation is highly altered by human activity. The natural  
124 vegetation is unknown but is thought to be Afromontane (Friis, 1992). Sources of non-  
125 aeolian contributions to their soils are unlikely to be more than 10 km distant at either AT or  
126 MM, and 20 km at AK. In general, the mantle of soil of the Plateau overtops Tertiary basalts  
127 associated with volcanism of the East African Rift. Further detail about lithology is provided  
128 in Gani et al., (2007), Gebru et al. (2009), and Terwilliger et al. (2011).

129

## 130 **2.2. Study section descriptions and sampling protocols**

131         One soil section per site was sampled for the full suite of proxies reported in this  
132 paper: AKIII (13° 19' 55.80" N, 39° 21' 52.56" E); MMII (13°35'1.05"N, 39°34'4.64"E); and ATI  
133 14° 16' 13.56" N, 39° 26' 52.18" E). AKIII and ATI are mineral soils distributed in layers of  
134 widely ranging textures and structures (Fig. 2, Appendix A). MMII is mostly older than 4500  
135 cal y BP reworked travertine and peat overtopped by very young mineral soil. Each section  
136 was excavated at least 1 m back from its wall. Sampling intervals were 10 cm or less for  
137 analyses of  $\delta^{13}\text{C}$  and percent total organic carbon of bulk organic matter. Compound specific  
138 isotopic, Rock-Eval pyrolysis, micromorphological, and total phosphorus analyses were  
139 made on selected samples of this collection. Selection criteria included even representation  
140 of time intervals followed by targeting of samples representing changes in soil morphology.

141 A separate sample set was obtained for radiocarbon dating, identification of charcoaled  
142 wood fragments, and descriptive analyses of soil characteristics such as texture, pH, and  
143 electrical conductivity. Protocols for soil sampling, drying, and storage prior to analyses are  
144 described further in Gebru et al. (2009) and Terwilliger et al. (2011).

145

### 146 **3. METHODS**

#### 147 **3.1. Land-plant derived fatty acid $\delta D$ analyses**

148 We analyzed  $\delta D$  values of long-chain ( $> n-C_{24}$ ) *n*-alkanoic (fatty) acids in this study  
149 because they were consistently more abundant than other *n*-alkyl lipid groups -- *n*-alkanes  
150 and *n*-alkanols -- that largely have land-plant sources (Eglinton and Hamilton, 1967;  
151 Kolattukudy, 1970). Extractions for analyses of  $\delta D$  values of specific, land-plant derived  
152 saturated fatty acids followed methods used in Huang et al. (2004). Specifically, total lipids  
153 were extracted from ca 12 g of soil per sample with 9:1 dichloromethane (DCM) and  
154 methanol (MeOH) at high temperature (120 °C) and pressure (1200 psi) using an accelerator  
155 solvent extractor (ASE 200, Dionex). Solid phase extraction columns (either Pasteur pipettes  
156 packed with aminopropyl or Supelclean™ LC-NH<sub>2</sub> SPE tubes) were used for elution of first,  
157 the neutral fraction (with DCM and isopropanol) and next, the fatty acids (with ether and  
158 acetic acid). Fatty acids were then dissolved in toluene, derivatized by methylation with  
159 MeOH of known  $\delta D$  acidified with acetyl chloride, and heated in closed vials at 60°C for 12 h.  
160 NaCl solution was then added to the methylated sample followed by liquid-liquid extraction  
161 using hexane. Fatty acid methyl esters (FAMES) were further purified through a silica gel  
162 column by first removing contaminants with hexane and then eluting the FAMES with DCM.

163 FAME  $\delta D$  values were analyzed by gas chromatography stable isotope mass  
164 spectrometry (GC-IRMS) that recognized compounds from the retention times of their peaks.  
165 FAME  $\delta D$  values of most AKIII and all of the MMII samples were obtained at Brown  
166 University by a GC (Agilent 6890) coupled to an IRMS (Finnigan Delta-plus XL) via a  
167 combustion module (Finnigan GC Combustion III). Concentrations were determined by Gas  
168 Chromatography-Flame Ionization Detection (GC-FID). The FAME  $\delta D$  values of samples

169 from ATI as well as some duplicate and additional samples from AKIII were obtained at  
170 Carnegie Institution on a GC (TRACE, ThermoFisher) coupled to an IRMS (Delta-plusXL,  
171 Thermo Finnigan) with a GC Combustion III interface. An HP1MS 30 m x 0.32 mm x 0.25  
172  $\mu\text{m}$  column was used at Brown University; a 60 m column at Carnegie Institution. In both  
173 GC-IRMS systems, samples were injected in pulsed splitless mode at 20 PSI for 1 min at a  
174 temperature of 320°C at Brown University and at 300°C at Carnegie Institution. Otherwise,  
175 GC running conditions were identical for the two systems.

176 An external standard with 6 peaks ( $n\text{-C}_{16}$ ,  $n\text{-C}_{18}$ ,  $n\text{-C}_{22}$ ,  $n\text{-C}_{24}$ ,  $n\text{-C}_{26}$ , and  $n\text{-C}_{28}$ ),  
177 calibrated against a certified standard often used in Huang's lab was used on both the Brown  
178 University and Carnegie Institution GC-IRMS systems. The standard errors in  $\delta\text{D}$  values  
179 were < 2.0 in each system. FAME  $\delta\text{D}$  values ( $\delta\text{D}_{\text{FAME}}$ ) were converted to  $\delta\text{D}$  values of their  
180 source compounds ( $\delta\text{D}_{\text{C}_S}$ ) by correcting for the 3 Hs from methylation ( $\delta\text{D}_{\text{MeOH}}$ ) via the mass  
181 balance approximation

$$182 \delta\text{D}_{\text{C}_S} = [\delta\text{D}_{\text{FAME}} - (3/n \delta\text{D}_{\text{MeOH}})] / [(n-3)/n] \quad [1]$$

183 where  $n$  denotes the number of hydrogen atoms in the specific source fatty acid. Mean  $\delta\text{D}$   
184 values of compounds in the standard differed by < 2.5‰ between laboratories, which was not  
185 statistically significant (t test,  $p \geq 0.2$ ).

186

### 187 3.2. Soil micromorphology and phosphorus contents

188 Thin sections were cut from 64 intact soil pedes from AKIII, MMII, and ATI to obtain  
189 quantitative microscopic image data about charred organic matter that are relevant to land  
190 clearing by fire. The samples were vapor-phase dried with acetone, then vacuum  
191 impregnated with polyester resin (Crystic 17449, Scott Bader PLC) according to standard  
192 methods at the University of Stirling ([www.thin.stir.ac.uk](http://www.thin.stir.ac.uk)). The resulting block was mounted,  
193 and sections cut, ground, and polished to 30  $\mu\text{m}$  thickness (as per Murphy, 1984; Adderley et  
194 al., 2002). Representative portions of each section were then selected by optical microscopy  
195 at x40–x200 magnification. Using different illumination methods, four sets of images were  
196 obtained from each portion via a polarized optical microscope, CCD camera, and imaging

197 software (AnalySIS, Olympus Optical Co.) at x80 magnification. These were: 1) transmitted  
198 plane polarized (ppl), 2) crossed-polarizers at 45° and 90° (xpl), 3) circularly polarized (cpl),  
199 and 4) reflected oblique incident illumination (oil).

200 Images were segmented using color and morphological criteria to distinguish charred  
201 organic matter (Adderley et al., 2002, 2010). First, pore space was identified by matching  
202 and comparing segments from the aforementioned cpl and xpl images; a process that  
203 eliminates the potential for mistaking basal-cut quartz grains for pores from the cpl images  
204 alone (Whalley et al., 2005). The methods of Simpson et al. (2003) were then extended to  
205 distinguish charred from other darkened materials, including peat, for the extremely wide  
206 range of soil colors and textures among our samples (Terwilliger et al., 2011). Our  
207 modification consisted of determining thresholds for charcoal-derived vs other organic  
208 materials by matching ppl and oil images and performing a set of pixel-level Boolean  
209 operations to distinguish the color (via ppl) and texture (oil) of charred from other dark  
210 materials. The total area attributable charred matter in each object was then recorded.

211 Total phosphorus content was analyzed to provide insights about anthropogenic  
212 impacts on landscapes on 10 g of ground soil from all samples that also provided peds for  
213 image analyses. These soils underwent acid-perfusate digestion followed by inductively  
214 coupled plasma- atomic emission spectroscopy (ICP-AES; Perkin Elmer Optima 5300DV)  
215 analyses (as per Association of Official Agricultural Chemists, 2000).

216

### 217 **3.3. Organic matter quality**

218 The state of preservation of organic matter was assessed from hydrogen (HI) and  
219 oxygen indices (OI) by Rock-Eval pyrolysis on an RE6 (Vinci Technologies)(rationales in  
220 Espitalié et al., 1985a; b; Disnar et al., 2003, 2008). HI is the mass of hydrocarbon-rich  
221 substances that is released during the pyrolysis phase of instrument operation, per mass of  
222 total organic carbon (TOC). OI is a measure of the oxygen content of the organic matter as  
223 given by the mass of O<sub>2</sub> in CO + CO<sub>2</sub> released during pyrolysis per mass TOC.

224

225 **3.4. Bulk C isotopic and elemental analyses, charcoal <sup>14</sup>C dating and identification**

226 Most bulk isotopic, carbon elemental, radiocarbon date and forest history data in this  
227 study have been published for other contexts. Further detail than that below about how they  
228 were obtained and analyzed are in Gebru et al. (2009) and Terwilliger et al. (2011).

229 Percent total organic carbon (%TOC) and  $\delta^{13}\text{C}$  values were obtained with an  
230 elemental analyzer (Carlo Erba NA 1500) coupled via continuous flow to a stable isotope  
231 ratio mass spectrometer (Conflo II to Delta XL plus, ThermoFinnigan). The  $\delta$  notation for the  
232 stable isotopic composition of each element (X) is defined by the equation

233 
$$\delta X = [(R_{\text{sample}}/R_{\text{standard}}) - 1] 1000 (\text{‰}) \quad [2]$$

234 where  $R = [^hX/^lX]$ , h = heavier isotope, l = lighter isotope, and the standard is Pee Dee  
235 Belemnite (Craig, 1957). The precision of the measurements was better than  $\pm 0.2\text{‰}$ .

236 The percentage of all ( $\text{C}_3 + \text{C}_4$ ) carbon from  $\text{C}_4$  plants in SOM ( $\%C_4$ ) was estimated  
237 using the equation (Trouve et al., 1994)

238 
$$\%C_4 = 100 (\delta^{13}\text{C}_{\text{SOM}} - \delta^{13}\text{C}_{\text{C}_3}) / (\delta^{13}\text{C}_{\text{C}_4} - \delta^{13}\text{C}_{\text{C}_3}) \quad [3]$$

239 The value used for  $\delta^{13}\text{C}_{\text{C}_3}$  was  $-29.09\text{‰}$  and  $-12.79\text{‰}$  for  $\delta^{13}\text{C}_{\text{C}_4}$ . These  $\delta^{13}\text{C}$  values were  
240 averages obtained from  $\text{C}_3$  and  $\text{C}_4$  plants collected at Debre-Zeit and Kulumsa agricultural  
241 experimental stations at similar elevation ranges to those of the study sites. The  $\%C_4$  values  
242 reported herein have no further corrections. Nonetheless, we considered and, where  
243 possible, modeled effects of a variety of factors other than photosynthetic pathway of plant  
244 sources that may influence  $\delta^{13}\text{C}_{\text{SOM}}$  values. These included Suess effect, decomposition, soil  
245 texture, and the correction that it would take to change a conclusion that  $\text{C}_4$  plants had  
246 dominated to an interpretation that  $>50\%$  of the vegetation had been  $\text{C}_3$  (details in Terwilliger  
247 et al., 2011). If all of these factors are considered,  $\%C_4$  estimates from [3] may be  
248 overestimated in all samples older than 150 cal y BP but the directions of changes in  $\%C_4$   
249 are likely robust.

250 Where present, charcoaled wood was obtained from soil samples by bucket flotation  
251 methods. Where possible, fragments were identified. This paper shows changes in relative  
252 compositions of gymnosperm (*Juniperus procera* forest communities) and angiosperm

253 (secondary forest or *Acacia* spp. woodland) trees. Charcoal was dated at the University of  
254 California at Irvine's Keck Carbon Cycle Accelerator Mass Spectrometry facility (Table 1).  
255 Radiocarbon ages were converted to calendar years before present (cal y BP, 1950 CE =  
256 present) using CALIB v5.0.2 (Stuiver and Reimer, 1986-2005) software and considerations in  
257 Stuiver and Reimer (1993). The median of the probability distribution for the calibration  
258 curve was used as a single estimate for the calendar age of a sample and was obtained from  
259 the aforementioned software. The median and the weighted average of the probability  
260 distribution of calibrated ages are the more robust of present single values for describing  
261 calendar age (Telford et al., 2004). Age-depth relationships for each section were  
262 determined by linear interpolation between charcoal dates with modifications suggested by  
263 changes in soil morphology.

264

### 265 **3.5. Soil physical and salinity description**

266 Additional analyses of soil physical characteristics informed sampling protocols,  
267 calculations of chronologies, and possible influences of salinity. These included field  
268 observations of changes in color, grain size, structure grade, and dry consistence using  
269 Munsell Soil Color Charts (1994) and guidelines in Schoeneberger et al. (2002). Soil texture  
270 was analyzed by a combination of dry sieving and the Bouyoucos (1936) hydrometer method  
271 with texture names following the United States Department of Agriculture classification (Soil  
272 Survey Staff, 1995). Soil pH and Electrical Conductivity (EC) were measured to assess  
273 salinity where soils with pH < 8.5 and EC > 4 were defined as saline where pH was  
274 measured by a potentiometer on soil suspended in water and EC water determined by the  
275 water saturated soil paste method (Rhoades, 1993). All texture, pH, and EC analyses were  
276 made by the Ethiopian National Soil Research Laboratory.

277

### 278 **3.6. Statistical analyses**

279 Data were examined for simple long-term trends over time with a maximum of one  
280 shift (optimal breakpoint) in those trends dividing a section into a maximum of two trend

281 segments using segmented line regression analyses (Draper and Smith, 1981; Thomson,  
282 1990). The optimal breakpoint for a shift was the point within the range of significant  
283 breakpoints with the largest coefficient of explanation (Oosterbaan et al., 1990). To cross-  
284 check or discretely discern environmental inferences, data from different pairs of proxies  
285 were examined for co-variation using correlation analysis that tested the Pearson's product-  
286 moment correlation coefficient for significance (Sokal and Rohlf, 1995).

287 Segmented regression analyses were performed using SegReg (Oosterbaan, no  
288 date). All other statistical analyses were performed using Minitab (version 13, State College,  
289 PA, USA). All statistical tests were considered to be significant at  $p \leq 0.05$ .

290

## 291 **4. RESULTS**

### 292 **4.1. Lithology, chronology, and salinity**

293 Together, the three sections spanned the last 8300 years and also represented a  
294 short time interval before ca 13,700 cal y BP (Table 1, Fig. 2). Dates were predominantly  
295 well-ordered. Soil layers varied markedly in texture and structure (Fig. 2, Appendix A) within  
296 sequences; facilitating the detection of hiati in time and changes in rates of net sedimentation  
297 for calculating time sequences. No hiatus in time was detected for ATI whereas AKIII and  
298 MMII each had one hiatus. If pedogenesis had occurred in any of the sections, however, it  
299 was very weak. Charcoal fragments were distributed regularly throughout the AKIII and ATI  
300 sections although the fragments were generally smaller and more fragile in AKIII. The deeper  
301 portion of the travertine/peat (ca 300–640 cm) and upper mineral layers of MMII contained  
302 abundant, large fragments of charcoaled wood but charcoaled wood fragments were not  
303 found in the upper (ca 100–300 cm) of this material (Fig. 2). Detailed explanations of how  
304 soil properties and charcoal distributions were used to enhance the interpolation of  
305 chronologies for each sequence are in Gebru et al. (2009) and Terwilliger et al. (2011).

306 Although all but one soil sample was basic, most were normal and not saline with pH  
307  $< 8.5$  and EC  $< 4.0$  dS m<sup>-1</sup> (Fig. 2). Nevertheless, most of the soil from the top of the  
308 reworked travertine/peat at 100 cm to 415 cm depth in MMII was saline. This included both

309 the portion where we could not find charcoaled wood and some of the portion where  
310 charcoaled wood fragments were abundant.

311

#### 312 **4.2. Specific fatty acid $\delta D$ and bulk organic $\delta^{13}C$ values**

313 The  $\delta D$  values of the fatty acids from land plant sources ( $n-C_{26}$ ,  $n-C_{28}$ ,  $n-C_{30}$ ) were  
314 significantly correlated to one another in each site (for  $n-C_{26}$  and  $n-C_{28}$  | AKIII:  $R=0.489$ ,  $p=$   
315  $0.011$ ; MMII:  $R=0.861$ ,  $p<0.0005$ ; ATI:  $R=0.975$ ,  $p<0.0005$ ), (for  $n-C_{26}$  and  $n-C_{30}$  | AKIII:  $R=$   
316  $0.540$ ,  $p=0.004$ ; MMII:  $R=0.715$ ,  $p<0.0005$ ; ATI:  $R=0.975$ ,  $p<0.0005$ ), (for  $n-C_{28}$  and  $n-C_{30}$  |  
317 AKIII:  $R=0.706$ ,  $p<0.0005$ ; MMII:  $R=0.851$ ,  $p<0.0005$ ; ATI:  $R=1$ ,  $p<0.0005$ )(Table 2).

318 Hereinafter, we focus only on the results for  $n-C_{26}$  as these consistently had the highest,  
319 most evenly-shaped peaks and the peaks were present in the most samples.

320  $\delta D_{n-C_{26}}$  values ranged from  $-172$  –  $-110\text{‰}$  in AKIII,  $-217$  to  $-126\text{‰}$  in MMII, and  $-153$  –  
321  $-127\text{‰}$  in ATI (Table 2).  $\delta D_{n-C_{26}}$  (but not  $\delta^{13}C$ ) values are very similar to one another among  
322 portions of the sections that overlap in time, although values from ATI never exceed those  
323 with closely corresponding ages in the slightly more arid, lower elevation AKIII (Fig. 3). In  
324 MMII, the section with most of the older than 4500 cal y BP values, a marked (40‰) shift  
325 (optimal breakpoint) to higher  $\delta D_{n-C_{26}}$  values occurred after ca 6035 cal y BP but much earlier  
326 than the point at which older reworked travertine/peat layers end and the very recent mineral  
327 soil layer begins (Table 3, Figs. 2, 3, 4). In AKIII, which has a hiatus from ca13700–4400 cal  
328 y BP,  $\delta D_{n-C_{26}}$  values increased linearly from oldest (ca 13750 cal y BP) to youngest (present)  
329 ages (Table 3, Fig. 5). In ATI,  $\delta D_{n-C_{26}}$  shifted to higher values after ca 2440 cal y BP (Table  
330 3, Fig.6). Furthermore,  $\delta D_{n-C_{26}}$  values decreased significantly from the oldest soil at ca 2750  
331 until 2440 cal y BP, then switched to increase to the youngest soils (ca 500 cal y BP) of that  
332 segment.

333 Similar trends in  $\delta^{13}C$  and  $\delta D_{n-C_{26}}$  values over time and positive correlations of  $\delta^{13}C$   
334 and  $\delta D_{n-C_{26}}$  would support the hypothesis that climate influenced changes in percentages of  
335 total organic carbon derived from  $C_4$  plants ( $\%C_4$ ). In MMII,  $\delta D_{n-C_{26}}$  and  $\delta^{13}C$  were correlated  
336 and also shifted to higher values after the same time (6035 cal y BP)(Fig. 4; Tables 3, 4).

337 Where they overlapped in time,  $\delta^{13}\text{C}$  values of bulk organic matter were more negative and  
338 thus  $\%C_4$  was lower in ATI than in the slightly more arid AKIII (Fig. 3). Nonetheless,  $\delta^{13}\text{C}$   
339 values were not correlated with  $\delta D_{n-C26}$  values in either AKIII or ATI. In contrast to  $\delta D_{n-C26}$ ,  
340  $\delta^{13}\text{C}$  of AKIII shifted to less negative values after ca 3435 cal y BP. However, values in the  
341 time segments before and after that date either did not vary linearly with time if the sample  
342 subset paired to  $\delta D_{n-C26}$  was used or increased significantly but slightly from older soils to the  
343 breakpoint, then decreased thereafter in the full data set (Fig. 5, Table 3). In ATI, the long-  
344 term trends in  $\delta^{13}\text{C}$  differed not only from those in  $\delta D_{n-C26}$  but also depending on whether the  
345 full or subset of data was examined (Fig. 6, Table 3). In the subset,  $\delta^{13}\text{C}$  values shifted to  
346 more negative values after ca 2110 cal y BP during a time segment when  $\delta D_{n-C26}$  values  
347 were increasing. In the full set,  $\delta^{13}\text{C}$  values decreased from older soils until shifting to less  
348 negative values at ca 2680 cal y BP, then decreased again thereafter.

349 In summary, long-term linear trends emerged within the  $\delta$  value sequences of each  
350 element. Large oscillations of relatively short duration occurred as well, however, regardless  
351 of whether or not there were significant long-term changes. Furthermore, although  
352 precipitation can influence the  $\delta$  values of both elements,  $\delta D_{n-C26}$  and  $\delta^{13}\text{C}$  values are only  
353 correlated in MMII (Table 4).

354

### 355 **4.3. Soil micromorphology, organic matter quality, elemental contents over time**

#### 356 *4.3.1. Mai Maikden*

357 Although shifts in values (at breakpoints) occurred in three of the five non-isotopic  
358 factors analyzed from MMII, the dates for shifts were unique to each factor (Fig. 4). Not  
359 surprisingly given its composition of peat and travertine as well as mineral soil layers (Fig. 2),  
360 percentages of organic carbon of total weight (%TOC) ranged more widely (0.4–8.5) and had  
361 larger short-term variations in MMII than in the other two sections (Table 2). Consequently  
362 the breakpoint dates for %TOC differed between tests of all available data (increase after ca  
363 7160 cal y BP) and data from the sample subset used for comparisons with other factors  
364 (decrease after 6280 cal y BP). Furthermore, when all data were examined, %TOC

365 decreased from older to younger soils during both the time segments prior to and following  
366 7160 cal y BP whereas data from the subset did not exhibit long term trends over the time  
367 segments before and after ca 6280 cal y BP. Hydrogen index values (HI) ranged from 0–163  
368 mg HC g<sup>-1</sup> TOC, decreased from older soils until ca 4915 cal y BP and then increased  
369 thereafter. Oxygen index values (OI) ranged from 236–423 mg O<sub>2</sub> g<sup>-1</sup> TOC, decreased from  
370 the oldest soil until ca 5880 cal y BP, increased greatly at that breakpoint, and then  
371 decreased thereafter. With a range from 89–890 mg P kg<sup>-1</sup>, Total phosphorus contents  
372 (Total P) were all lower in MMII than elsewhere. Total P increased from older to younger  
373 soils. In contrast, although the percent area that consisted of charred organic matter  
374 (%Char) ranged greatly from 0–68 and shifted by > 50 % over several short time intervals,  
375 there were no trends in %Char over the long term.

376

#### 377 4.3.2. *Adi Kolan*

378 In addition to the  $\delta$  values, significant shifts in three of the five non-isotopic soil  
379 analyses occurred at ca 3435 cal y BP in AKIII (Fig. 5) suggesting a simultaneous influence  
380 of environmental change at that time. %TOC, which ranged from 0.1–2.2 (Table 2), was  
381 higher after than before that date. OI decreased significantly after 3435 cal y BP and  
382 increased from older to younger soils over the time segments before and after that date. OI  
383 values ranged from 265–741 mg O<sub>2</sub> g<sup>-1</sup>TOC. Total P also shifted from higher values before  
384 to lower values after 3435 cal y BP; decreasing from older to younger soils during the time  
385 segment prior to that date and increasing towards the present time thereafter. Total P  
386 values ranged from 1133–1976 mg P kg<sup>-1</sup> in AKIII and were the highest of the three sections.

387 HI values in AKIII ranged from 0–80 mg HC g<sup>-1</sup> TOC, decreased significantly if <1 mg  
388 HC g<sup>-1</sup> TOC from the oldest soils until ca 2750 cal y BP, and then increased thereafter. The  
389 percent area that consisted of charred material (%Char) was lower after ca 2200 cal y BP  
390 than before. %Char ranged from 0.4–50 (Table 2).

391

#### 392 4.3.3. *Adigrat*

393 Shifts in values occurred in three of the soil factors measured in ATI but the  
394 breakpoints differed among factors (Fig. 6). When all of the available data were analyzed,  
395 %TOC was significantly higher after ca 2275 cal y BP than before that date. When only the  
396 subset of values for samples matching other factors was examined, %TOC increased from  
397 older to younger soils without a breakpoint. The total range in %TOC from 0.1–1.5, was the  
398 smallest of the three sites (Table 2). HI values ranged from 0–104 mg HC g<sup>-1</sup> TOC and  
399 increased from older to younger soils. OI values ranged from 375–875 mg O<sub>2</sub> g<sup>-1</sup> TOC, and  
400 changed from a faster rate of decrease from older soils until ca 2180 cal y BP to a slower  
401 rate of decrease thereafter. Total P ranged less in value (974–1034 mg P kg<sup>-1</sup>) than  
402 elsewhere and exhibited no significant long-term changes. %Char, which ranged in values  
403 from 0.9–13.8, shifted to higher values at ca 2100 cal y BP and values decreased from older  
404 to younger soils during both the time segments prior to and after that date.

405

#### 406 **4.4. Correlations between proxies**

407 Of all possible comparisons of proxies, only two factors; OI and %TOC, were  
408 significantly correlated (negatively) with one another in all three sites (Table 4). Furthermore,  
409 factors that are commonly correlated did not co-vary in all three sites. For example, HI and  
410 OI are commonly negatively correlated with HI decreasing and OI increasing with  
411 humification (Disnar et al., 2003). Although HI and OI were negatively correlated in MMII and  
412 ATI, they were unrelated to one another in AKIII. These results suggest that each factor is  
413 discretely influenced by environment and that there were differences in the precise suite of  
414 environmental changes that occurred among sites.

415

## 416 **5. DISCUSSION**

### 417 **5.1. Evaluation of δD leaf wax fatty acids as a proxy for precipitation**

418 The source of hydrogen for any organic compound in a plant is water used in  
419 photosynthesis (Ruben et al., 1941). The original source of that water is precipitation and  
420 climate influences its δD value (Dansgaard, 1964; Yurtsever, 1975; Gat, 1980; Vimeux et al.,

421 1999). At tropical latitudes such as those of our sites, precipitation occurs in closest  
422 proximity to the bulk of global cloud formation and its  $\delta D$  values are most influenced by its  
423 amount.  $\delta D$  values decrease as precipitation amount increases (Risi et al., 2008). Additional  
424 factors shape the  $\delta D$  values of fatty acids in land-plants as well but their consideration below  
425 suggests that our  $\delta D_{n-C26}$  sequences were unambiguously if qualitatively reflecting changes  
426 in amount of precipitation.

427 Elevation, distance from the ocean, and the fraction of global water in ice can also  
428 affect the  $\delta D$  values of precipitation. Any effect of distance on  $\delta D_{n-C26}$  values in our study  
429 was likely constant as our sites are virtually equidistant from their oceanic source of  
430 precipitation. The tendency for  $\delta D_{n-C26}$  values in ATI to be similar to but never greater than  
431 those from the overlapping time interval in AKIII may be a result of differences in elevation  
432 and/or amount of precipitation. A correction curve for the effects of changes in ice volume  
433 over the last 44,000 years on  $\delta D$  values of *n*-alkanes in West African marine sediments  
434 (Niedermeyer et al., 2010) suggests that differences in ice volume would only have affected  
435 the  $\delta D_{n-C26}$  value of our oldest sample (ca 13,750 cal y BP at AKIII, Figs. 3, 5); lowering it by  
436 < 5‰.

437 Plant to plant differences in fractionations between  $\delta D$  values of *n*-alkyl compounds  
438 and their precipitation source may introduce the greatest error in interpreting rainfall amount.  
439 Most findings from this active area of study have been on *n*-alkanes but are probably equally  
440 applicable to fatty acids (Chikaraishi and Naraoka, 2003, 2007; Chikaraishi et al., 2004).  
441 Evaporation gradients tend to cause water to be more D-enriched at the surface of soils than  
442 at depth. As a result, differences in  $\delta D$  values of *n*-alkyl compounds among plant species  
443 growing in the same area may reflect differences in the depths at which their roots take up  
444 water (e.g., Krull et al., 2006). Evapotranspiration may cause the leaf water used in  
445 photosynthesis to be D-enriched compared to its precipitation source (Sternberg, 1989;  
446 Yakir, 1992), resulting in a magnification of the inverse relationship between  $\delta D$  values and  
447 amount of precipitation (Worden et al., 2007). Effects of evapotranspiration on  $\delta D$  values of  
448 leaf water may differ among plant types (Jackson et al., 1999; Smith and Freeman, 2006;

449 Feakins and Sessions, 2010a; Enquist and Enquist, 2011).

450 Hydrogen isotopic fractionations also occur during biochemical reactions leading to *n*-  
451 alkyl compound synthesis. Particularly large hydrogen fractionations occur during  
452 photosynthesis, metabolism, and when reactants include organic compounds that are not  
453 immediate outputs from photosynthesis (photoheterotrophic or heterotrophic) (Estep and  
454 Hoering, 1980, 1981; Sessions et al., 1999; Zhang et al., 2009). The net result of these  
455 factors was thought to be a virtually constant total biochemical fractionation for lipids  
456 (Sternberg et al., 1984). Recent findings of different  $\delta D$  *n*-alkane values among plants with  
457 different photosynthetic pathways that could not be explained by differences in  
458 evapotranspiration have led to the recognition that combined biochemical fractionations can  
459 no longer be assumed constant among plant types (Feakins and Sessions, 2010b; Polissar  
460 et al., 2010; McInerney et al., 2011).

461 In addition to the similarity in  $\delta D_{n-C26}$  values at similar ages in AKIII and ATI, two lines  
462 of evidence suggest that our  $\delta D_{n-C26}$  data unambiguously if perhaps qualitatively reflect  
463 changes in precipitation despite potentially confounding influences of vegetation type and  
464 other factors. First, larger changes in  $\delta D_{n-C26}$  correspond in time to dry and wet intervals  
465 indicated by proxies in lake sediments of eastern Africa. Second, consideration of influences  
466 of vegetation changes to  $\delta D_{n-C26}$  values does not alter the direction of implied precipitation  
467 trends.

468 The significant shift to higher  $\delta D_{n-C26}$  values after ca 6035 (MMII, Table 3, Fig. 4) is an  
469 example of the first line of evidence above as it fits the time range for the end of the East  
470 African humid period from a wide range of proxies in lakes and oceanic sediments (e.g.,  
471 Gasse, 2000; Nyssen et al. 2004, Marshall et al., 2009, 2011; Tierney et al., 2011). Dramis et  
472 al. (2003) based the timing of the increase in aridity on the end of travertine/peat layer  
473 formation at Mai Maikden and other nearby gullies that, like MMII was closer to ca 4500 cal y  
474 BP. The  $\delta^{13}C$  values at MMII shifted to less negative values at the same time as the shift in  
475  $\delta D_{n-C26}$  favoring the interpretation that decreasing precipitation contributed to a relative  
476 increase in  $C_4$  plant cover. The moderate salinity of soils during the time of the shift could

477 have favored C<sub>4</sub> plants in any autochthonous inputs but unless our data are skewed by  
478 leaching, MMII had become saline well before the change in  $\delta^{13}\text{C}$  values (Fig. 2). Factors  
479 other than photosynthetic pathway such as algal input and physical soil properties apparently  
480 had a negligible effect on the variation in  $\delta^{13}\text{C}$  values of bulk soil organic matter so the best  
481 supported explanation for the shift in  $\delta^{13}\text{C}$  values is that the proportion of biomass in C<sub>4</sub>  
482 plants increased at that time (Gebru et al., 2009; Terwilliger et al., 2011).

483         Although not systematic in direction over time, considerable variation in  $\delta\text{D}_{n\text{-C}26}$  (and  
484  $\delta\text{D}_{\text{C}3}$ ) values in MMII occurred during the generally wetter period before ca 6000 cal y BP  
485 (Table 2; Fig. 4). The most marked oscillation from the mean for this period consisted of a  
486 large (64‰) increase that peaked at ca 7400 cal y BP. This increase closely corresponds to  
487 inferences of a dry period including this time from a variety of lacustrine microfossil proxies in  
488 eastern Africa (e.g., Stager and Mayewski, 1997; Chalié and Gasse, 2002) and supports the  
489 conclusion about magnetic and geochemical data from Lake Tana in Ethiopia that the  
490 duration of the dry period peaking at that time was short (Marshall et al., 2011).

491         The largest excursion in  $\delta\text{D}_{n\text{-C}26}$  values after the end of the East African Humid Period  
492 occurs as a 35‰ increase beginning after 3800 and peaking at ca 3550 cal y BP in AKIII  
493 (Table 2; Fig. 5). Furthermore, magnetic susceptibility data at Lake Tana suggest that a dry  
494 period of similar duration began at 4200 cal y BP (Marshall et al., 2011). In addition, the  
495 timing of the dry period implied by our  $\delta\text{D}$  results is within the longer dry interval implied by  
496 valley infill characteristics elsewhere in the territory of D'MT and the Aksumite (Machado et  
497 al., 1998). Finally, this implied dry period is compatible in time with dry periods inferred for  
498 Italy, lake regions of eastern Africa, and that have been associated with the fall of  
499 sophisticated Akkadian and Egyptian cultures (Weiss et al., 1993; Hassan, 1997; Cullen et  
500 al, 2000; Gasse, 2000; Drysdale et al., 2006).

501         The second line of evidence that trends in our  $\delta\text{D}_{n\text{-C}26}$  values unambiguously reflect  
502 changes precipitation amount is that the effects of vegetation on these values, to the best of  
503 current knowledge; do not alter the direction of these trends. Our data thus far imply large  
504 changes in forest types as well as in relative inputs of herbaceous C<sub>4</sub> plants (Figs. 4–6).

505 The largest reported difference in  $\delta D$  of an  $n$ -alkyl compound between plant groups that  
506 could have led to faulty inferences about changes in precipitation in our study sections is a  
507 21 ‰ D enrichment in  $C_4$  compared to  $C_3$  grasses (Smith and Freeman, 2006; McInerney et  
508 al., 2011). We evaluated the role of change in relative contributions of  $C_4$  cover on  
509 inferences about climate by estimating what the  $\delta D_{n-C26}$  values of each sample would be if it  
510 consisted entirely of  $C_3$  grass sources ( $\delta D_{C3}$ ) according to the following equations.

$$511 \quad \delta D_{n-C26} \text{ measured} = \rho(\delta D_{C4}) + (1-\rho)(\delta D_{C3}) \quad [4]$$

$$512 \quad \text{and } \delta D_{C4} = \delta D_{C3} + 21 \quad [4a]$$

513 where  $\rho$  = the proportional contribution by  $C_4$  plant sources (as calculated from [3]). Other  
514 than being lower, estimated  $\delta D_{C3}$  values had similar trends to those found for measured  $\delta D_{n-}$   
515  $c_{26}$  values (Table 2). Statistically,  $\delta D_{n-C26}$  values increased by 40‰ on average from before to  
516 after ca 6035 cal y BP whereas  $\delta D_{C3}$  values increased by 38‰ from before to after ca 5880  
517 cal y BP in MMII. Whereas the change in  $\delta D_{n-C26}$  values from start to peak of the implied  
518 drier interval prior to ca. 6000 cal y BP at MMII was 64 ‰, the corresponding change in  $\delta D_{C3}$   
519 was a negligibly larger 67 ‰. The magnitude of the change from start to peak of the largest  
520 dry interval after ca. 6000 cal y BP in AKIII was the same (35 ‰) for both  $\delta D_{n-C26}$  and  $\delta D_{C3}$ .

521 Moreover, it is possible that effects of vegetation type mask an even larger decrease  
522 in precipitation at ca. 6000 cal y BP than indicated by the aforementioned raw and modeled  
523  $\delta D$  values. The literature on whether  $\delta D$  values of  $n$ -alkyl groups vary systematically between  
524 woody and herbaceous plant community types is presently less consistent and subject to  
525 environmental control than the literature comparing  $\delta D$  values of  $C_3$  and  $C_4$  grasses (Bossard  
526 et al., 2011). Given that constraint, average  $\delta D$  values of  $n$ -alkanes and fatty acids of  $C_4$   
527 grasses (monocots) have been found to be lower than or similar to  $C_3$  gymnosperms and  
528 dicotyledonous angiosperm tree species (e.g. for  $n$ -alkanes, Chikaraishi and Naraoka, 2003;  
529 Krull et al., 2006; for fatty acids, Chikaraishi et al. 2004).

530 Together with higher  $\delta^{13}C$  values, an absence of charcoaled wood at MMII suggests  
531 that  $C_4$ -plant vegetation cover increased relative to that of  $C_3$  plants following the  $\delta D_{n-C26}$  shift  
532 at ca 6035 cal y BP (Fig 4). The combination of lower  $\delta^{13}C$  values and continuous record of

533 both angiosperm and gymnosperm forest suggest that forest comprised a significant  
534 component of the C<sub>3</sub> vegetation prior to ca 6035. Correction of this component to  $\delta D$  values  
535 of a comparable proportion of C<sub>3</sub> grasses would result in inferences of even wetter times  
536 during the East African Humid period than our raw data suggest. The dry interval during the  
537 East African Humid period seems to have been accompanied by a switch from Angiosperm  
538 tree species dominant forests to gymnosperms species dominant forests or an equal mixture  
539 of both forest types. If present indications that gymnosperm trees may have higher  $\delta D$  *n*-  
540 alkyl compound values than angiosperm trees are universally correct, then the magnitude of  
541 the dry interval was lower than suggested by the raw  $\delta D_{n-C26}$  value record. Present  
542 indications are that if there are systematic differences in  $\delta D_{n-C26}$  between gymnosperms and  
543 angiosperm trees, they are not nearly large enough to erase or oppose to implication of a  
544 drier interval at ca 7400 cal y BP from the MMIII record. There is no indication of significant  
545 forest cover in AKIII so no further indication of vegetation influences on the dry interval  
546 peaking at ca 3550 cal y BP implied by the  $\delta D_{n-C26}$  record there.

547         There is consensus that drier and wetter periods followed the ca 3550 cal y BP dry  
548 interval but the timing of those periods remains contentious for the Plateau (Nyssen et al.,  
549 2004). As synthesized in the following section, together with our other proxies,  $\delta D_{n-C26}$   
550 values promise more developed conclusions about the relative importances of precipitation  
551 and land clearing during the times of the Plateau's most powerful civilizations than were  
552 possible from other proxies that have been employed in the region.

553

## 554 **5.2. Environmental change and the rise and fall of D'MT and the Aksumite**

555         The  $\delta D$  analyses suggest that decreases in precipitation peaking at ca 7400 and  
556 3550 cal y BP as well at the end of the East African Humid Period were greater than any long  
557 or short-term trends during or following the times of D'MT and the Aksumite. Our results also  
558 suggest that if there has been a long term drying trend (significant increase in  $\delta D$ ) since the  
559 end of the East African Humid Period, it has been slight and possibly only during the last  
560 2500 years. The predicted (from segmented regression equation) increase in  $\delta D$  at AKIII --

561 the site with the longest continuous post-Humid Period chronology-- from ca 4400 cal y BP to  
562 the present was a small 12 (for  $\delta D_{C3}$ )–14‰ (for  $\delta D_{n-C26}$ ) (Tables 2, 3; Fig. 5). In ATI,  $\delta D$   
563 values significantly increased over time but only after ca 2440 cal y BP (Tables 2, 3; Fig. 6).  
564 Changes in predicted  $\delta D$  values from 2440 cal y BP to the present are slight and similar in  
565 AKIII and ATI despite different vegetation histories. Specifically, the predicted increase over  
566 this time interval was 6.5 (for  $\delta D_{C3}$ )–8.0 ‰ ( $\delta D_{n-C26}$ ) in AKIII and 7.4 ( $\delta D_{n-C26}$ )–10.8‰ ( $\delta D_{C3}$ )  
567 in ATI. Differences in predicted  $\delta D$  values between AKIII and ATI are small at any given  
568 time, ranging from 8.0–8.6‰ for  $\delta D_{n-C26}$  and further reduced to range from 1.0 –3.2‰ for  
569  $\delta D_{C3}$ .

570 The  $\delta D$  records do suggest that relatively wetter and drier short-term intervals  
571 occurred during the times of D'MT and the Aksumite and that the changes in precipitation  
572 during these intervals was greater than over any long-term period following the East African  
573 Humid Period (Figs. 2, 5 and 6). Most notably, the emergences of both civilizations occurred  
574 within modestly wetter intervals of short duration. Therefore, higher rainfall cannot be  
575 discounted as an influence on the rise of the civilizations. No single pattern describes the  
576 changes in precipitation during the declines of both civilizations, however.

577 Land clearing dynamics can also contribute to the complexity of polities. As indicated  
578 in the following subsections, our results suggest different controls on land clearing and  
579 different relationships between climate and land clearing at different times and places.

580

### 581 *5.2.1. Land clearing, human influence at Mai Maikden*

582 Most trends in bulk carbon isotopic, elemental, and soil micromorphological factors at  
583 MMII could have occurred with time and/or with changes in precipitation amount as inferred  
584 from  $\delta D$  values (Fig. 4). Land clearing and other decreases in biomass are possible  
585 influences on these trends as well but are weaker than climate and time.

586 The relative increase in  $C_4$  vegetation with decreasing rainfall at tropical latitudes has  
587 been attributed to the increased advantage of conserving water that also limits access to  
588 atmospheric  $CO_2$  (Teeri, 1988).  $C_4$  plants maintain high concentrations of  $CO_2$  for productive

589 photosynthetic uptake while virtually eliminating energy consumptive photorespiration (Hatch,  
590 1978). The added energy costs of C<sub>4</sub> photosynthesis are compensated for in environments  
591 where photorespiration rates would otherwise be high due to depleted CO<sub>2</sub> concentrations  
592 (Nobel, 1999). The concurrent increases in δD and δ<sup>13</sup>C values at the end of the East  
593 African Humid Period at MMII are consistent with the explanation that the shift to a drier  
594 climate favored C<sub>4</sub> over C<sub>3</sub> plants (Fig. 4). Similarly, the correlation between δD and δ<sup>13</sup>C  
595 values throughout MMII (Table 4) is consistent with the favoring of C<sub>4</sub> over C<sub>3</sub> plants as  
596 rainfall decreases.

597 Trends in % area of charred organic matter (%Char Fig. 4) indicate that fire was a  
598 significant component of Mai Maikden's land clearing history. The following lines of evidence  
599 suggest that this history is not one of severely hot fires and furthermore that changes in  
600 vegetation were most strongly linked to climate prior to the hiatus in the MMII time sequence  
601 (before ca 4500 cal y BP). First, hydrogen (HI) and oxygen (OI) indices from Rock-eval  
602 pyrolysis are negatively correlated suggesting that chemical changes in organic matter were  
603 caused by oxidative processes such as humification (Lafargue et al., 1998; Disnar et al.,  
604 2003) and/or fire of low thermal intensity. HI decreases as organic matter becomes altered,  
605 while the accumulation of products from oxidation causes OI to increase. During fires of high  
606 thermal severity, these products may be combusted resulting in lowered OI (Rein et al.,  
607 2008).

608 Second, the combined absence of macroscopic wood fragments, low percentages of  
609 TOC, and shift to higher %C<sub>4</sub> plants in the vegetation biomass (Figs. 2, 4) suggest that Mai  
610 Maikden had negligible forest cover from the end of the East African Humid Period to ca  
611 4500 cal y BP and that the high %Char was herbaceous in origin. Although fire may have  
612 helped to maintain the deforested condition, the shift in vegetation and precipitation (at ca  
613 6000 cal y BP) occurred prior to evidence from %Char for increased burning (at ca 5600 cal  
614 y BP).

615 Finally, the vegetation history of MMII prior to 6000 cal y BP includes a continuous  
616 presence of closed canopy, fire intolerant juniper forests (gymnosperms in Fig. 4) and a

617 more intermittent presence of comparatively open canopy, fire and drought tolerant species  
618 such as *Acacia abyssinica* (Gebru et al., 2009 and angiosperms in Fig. 4). The combination  
619 of the two ecosystems further suggests that fire was never of sufficient thermal severity to  
620 completely clear the juniper forests of the East African Humid Period.

621 The pre-hiatus period at MMII predates D'MT—the earliest of the Plateau's known  
622 kingdoms. The lack of relationship between  $\delta D$  (precipitation) and %Char (fire) suggests that  
623 factors other than climate, per se, influenced fire patterns. A role of humans in land clearing  
624 then cannot be discounted, however. Land clearing by fire has been an integral practice of  
625 most ancient agricultural societies and genetic and linguistic (but not radiocarbon) analyses  
626 suggest that agricultural societies predated D'MT in the Plateau by thousands of years  
627 (Bellwood, 2005; Harrower et al., 2010).

628 Soils after the hiatus in MMII were younger than ca 150 cal y BP. Identified  
629 charcoaled wood indicates that the surrounding area was more forested than at either the  
630 period from ca 6000–4500 cal y BP or in today's almost entirely deforested landscape  
631 (Gebru et al., 2009). Some juniper forest remained but *Acacia* woodlands were clearly more  
632 dominant than during the East African Humid Period. Although the climate had not become  
633 too dry to support juniper forest types, climate may have influenced the change in vegetation  
634 in addition to fire patterns that continue to suggest low thermal severity. The %Char values  
635 were lower than their maximums during dry or wet portions of the pre-hiatus time interval.  
636 The relatively high HI in conjunction with low OI suggests that the organic matter had  
637 experienced minimal decomposition or burning (Disnar et al., 2003)(Fig. 4).

638 At no time does the total phosphorus content (Total P) record suggest intensive  
639 human influences such as urbanization or manure and fuel residue-based agriculture  
640 (Simpson et al., 2002; Adderley and Simpson, 2005; Edwards et al., 2005; Adderley et al.,  
641 2006, 2008, 2010; Filippelli et al., 2010). Agricultural activity was most likely during the time  
642 of the young, pre-hiatus soils. Total P was highest in the young mineral soil at Mai Maikden  
643 but was still lower than at the other two sites. Therefore, if there were agriculture, it did not  
644 include significant human effort to manipulate soil fertility. The older soils were reworked

645 travertine and peat which are typically P depleted in comparison to mineral soils (Richardson,  
646 1985). Time and change in soil type may fully explain why Total P was highest in the  
647 youngest soils of MMII.

648

#### 649 5.2.2. *Land clearing, human influence at Adigrat*

650 Unlike the Mai Maikden sequence, there is no evidence that changes in rainfall had a  
651 dominant, long-term influence on %C<sub>4</sub> plant biomass or any other factor at Adigrat (Table 4).  
652 Land clearing with possible anthropogenic input may be a reason that %C<sub>4</sub> was not  
653 correlated with climate. Not only precipitation, but also land clearing can create conditions  
654 that favor C<sub>4</sub> over C<sub>3</sub> plants (Stowe and Teeri, 1978) and anthropogenic land clearing  
655 practices can affect %C<sub>4</sub> more than rainfall in the Ethiopian Highlands (Eshetu and Högberg,  
656 2000; Eshetu, 2002; Terwilliger et al., 2008). During the time of D'MT, %C<sub>4</sub> was considerably  
657 more variable than throughout the rest of the ATI chronology (Fig. 6) and this variability may  
658 best reflect rapid changes in land clearing.

659 Fire clearly contributed to the land clearing dynamics at Adigrat although our results  
660 suggest that fires tended to be of low thermal severity. Fire was a nearly continuous element  
661 of ATI's history as macroscopic charcoal fragments were present in all but one soil sample  
662 (Fig. 2). Furthermore, changes in tree species' composition are consistent with fire history,  
663 not rainfall. Adigrat had the most favorable climate for fire-intolerant juniper forest types but  
664 although *Juniperus procera* fragments occurred in all soils sampled for charcoal, fire-tolerant  
665 *Acacia abyssinica* was a significant component of the charcoal in all but one soil sample as  
666 well (Gebru et al., 2009; Terwilliger et al., 2011). As at Mai Maikden, the negative  
667 relationship between HI and OI at Adigrat (Table 4) could be caused by chemical changes  
668 during humification and/or fire of low thermal intensity. Time alone could have caused HI to  
669 decrease with age (Fig. 6). The increased rate of change of OI during the time of D'MT may  
670 have been caused by fires of low thermal severity, although the direction of change in OI with  
671 time then could be a consequence of decomposition alone.

672 Although anthropogenic activities likely explain why changes in vegetation seem to be

673 more related to land clearing than to climate; human impacts were probably light. In addition  
674 to the signs that fires were of low thermal severity, %Char and %TOC were consistently too  
675 low and invariant at Adigrat to suggest that humans had manipulated them to amend soil.  
676 Total P was higher and may indicate a higher human influence at ATI than at Mai Maikden.  
677 Total P varied little with time, however, suggesting that human impacts on soil fertility did not  
678 intensify during the times of the D'MT and Aksumite peoples.

679

### 680 5.2.3. Land clearing, human influence at Adi Kolen

681 No long-term relationships were found between precipitation ( $\delta D_{n-C26}$ ) and other  
682 proxies at Adi Kolen (Table 4, Fig. 5). Instead, land-clearing pressures probably most  
683 influenced some shorter-term changes in proxy values, particularly around the time of D'MT.

684 Charcoalized wood was found throughout the Adi Kolan sections suggesting a long  
685 history of fire (Geburu et al., 2009; Terwilliger et al., 2011). The few charcoal fragments that  
686 could be identified indicated that some fire-intolerant juniper forest existed recently.

687 Somewhat more arid climate may have contributed to the higher %C<sub>4</sub>, less forested  
688 surroundings at Adi Kolen than at Adigrat (Figs. 3, 5, 6). Otherwise, most of the change in  
689 %C<sub>4</sub> during AKIII's post-hiatus history (ca 4500 cal y BP to the present) is more consistent  
690 with land clearing, at times including intensified human activity, rather than a climatic  
691 explanation.

692 The shift to higher %C<sub>4</sub> after ca 3435 cal y BP occurred during the drier interval but  
693 more than a century after the peak  $\delta D$  value at ca 3550 cal y BP (Fig. 5). This was not a lag  
694 in response because %C<sub>4</sub> increased continuously even as precipitation increased until the  
695 beginning of the rise of D'MT. The simultaneous shift in other factors further suggests that  
696 the increase in %C<sub>4</sub> has other causes than climate. First, the higher %TOC in conjunction  
697 with increasing  $\delta D_{n-C26}$  values suggests a wetter environment that could produce more  
698 biomass to burn. Second, the sharp increase in %Char indicates that fire-contributed matter  
699 increased in the %TOC, while also creating conditions favoring C<sub>4</sub> plants by clearing land.  
700 The sudden drop in OI at ca 3435 cal y BP is coupled with negligible HI values suggesting

701 that the organic matter was severely altered chemically but not by decomposition. Fire of  
702 higher thermal severity could produce the combination of both low HI and OI (Fig. 5).

703 The increase of organic matter altered by means other than humification and rich in  
704 charred sources persisted until close to the end of D'MT's time. Human manipulation alone  
705 is consistent with these results whereas there are no clear other mechanisms for producing  
706 this unusual suite of conditions. Total P was generally highest and most variable at Adi  
707 Kolan. Since this includes high values prior to ca 13500 cal y BP, it is doubtful that human  
708 influences are responsible for the abundance of Total P at Adi Kolan relative to the other  
709 sites. Nonetheless, Total P shifted to lower values at ca 3435 cal y BP, increased markedly  
710 close to the rise of D'MT, and fell in tandem with %Char and %TOC close to D'MT's decline.  
711 Total P may rise or fall as a function of fire frequency and thermal intensity (Galang et al.,  
712 2010; Resende et al., 2011). A combination of changes in fire regime and human responses  
713 to problems associated with the early drop in phosphorus may have contributed to the  
714 changes in Total P during this time.

715 Whether or not humans were involved, our results suggest that developments related  
716 to land clearing differed between the times of D'MT and the Aksumite at Adi Kolan: %C<sub>4</sub>  
717 changed little during the time of Aksum, and %TOC was low as was the contribution of  
718 charred matter to it. The combined decrease in HI with time and stable, relatively high OI  
719 could be explained by humification and/or a regime of low thermal severity fire. There is no  
720 evidence, however, that the landscape was becoming heavily forested.

721

## 722 **6. CONCLUSIONS**

723 Combined analyses of  $\delta D$  values from land-plant derived fatty acid compounds (*n*-  
724 C<sub>26</sub>, C<sub>28</sub>, C<sub>30</sub>) and other soil proxies in northern Ethiopia provided discrete insights about  
725 climate and land clearing relevant to the times of two ancient civilizations --D'MT and the  
726 Aksumite Empire. Three results suggested that the  $\delta D$  values yielded unambiguous records  
727 of changes in precipitation that are critical for discerning land clearing characteristics from  
728 other proxies. One showed our  $\delta D_{n-C26}$  values to increase at times of droughts obtained from

729 studies of eastern African lakes. Another showed  $\delta D_{n-C26}$  values in different sites to co-vary  
730 during the same time intervals. Finally, correcting for one of the largest effects of plant type  
731 on  $\delta D$  values of *n*-alkyl group molecules did not change trends in  $\delta D_{n-C26}$  values with time.

732         Rainfall ( $\delta D_{n-C26}$ ) was highest and changed the most prior to ca 6000 cal y BP. Within  
733 that context, both D'MT (ca 2750–2350 cal y BP) and the Aksumite (ca 2100–1250 cal y BP)  
734 arose during wetter intervals of their relatively stable and arid times. In the two sites (AKIII  
735 and ATI) with time sequences spanning both civilizations,  $\delta^{13}C$  values of bulk organic matter  
736 were unrelated to precipitation suggesting that land clearing was a more important influence  
737 than climate on relative biomasses of  $C_4$  and  $C_3$  plants. Charcoalized wood fragments  
738 spanning long time periods in both sites suggest fire was an important agent of land clearing.

739         The % $C_4$  plant biomass varied more during the time of D'MT than during the Aksumite  
740 in both sites. Otherwise, our results suggest that characteristics of land clearing differed  
741 between the two sites. Hydrogen (HI) and oxygen (OI) indices were negatively related in ATI  
742 indicating that chemical alterations of organic matter were due to humification and/or fire of  
743 low thermal severity. Total phosphorus contents (Total P) varied little with time and so were  
744 not affected by intensified human activity specific to the support of the civilizations.

745         Our results for AKIII suggest that relatively high human impacts and fires of high  
746 thermal severity affected the time of D'MT but not the Aksumite. In contrast to ATI, HI was  
747 positively related to OI at AKIII. In particular, from ca 3435 to the time of D'MT's decline,  
748 negligible HI indicative of severely altered organic matter was coupled to the lowest OI  
749 values of our entire data set, negating the buildup of oxidized products associated with  
750 humification as a cause of that alteration. Moreover, % $C_4$  plant biomass increased with  
751 decreasing precipitation and %total organic carbon as well as the contribution of charred  
752 matter to it were high relative to the rest of AKIII's time sequence. An increased role of fire  
753 sustained by human manipulation would produce these results. An increase in Total P  
754 spanning the time of D'MT may further signal human manipulation of the landscape. The  
755 time of the Aksumite suggested less severe changes in land clearance with higher OI relative  
756 to HI and much lower %TOC, %Charred matter, and Total P.

757           The history of a succession of highly complex human polities makes the study region  
758 a valuable natural system for testing hypotheses about repeatability of relationships between  
759 environmental change and the status of civilizations. Although data are now needed closer  
760 to ancient urban population centers and at higher time resolution, our results suggest that  
761 some environmental changes may be more repeatable than others. The rise of both D'MT  
762 and the Aksumite occurred during relatively wet intervals of the driest, least climatically  
763 variable portion of the Holocene. Land clearance history apparently varied between the two  
764 civilizations and between locations within their boundaries.  
765

766 **Acknowledgements**

767

768 We dedicate this paper to the memory of Mohammed Umer who provided guidance in the  
769 selection of field sites and contributed intellectually to many aspects of the research.

770 Terwilliger thanks Li Gao, then at Huang's lab, for teaching her and Tsige Gebru Kassa  
771 methods for extracting fatty acids from the soil samples and to Tsige Gebru Kassa for

772 assistance with those extractions. Terwilliger also thanks Ying Wang and Roxane Bowden

773 for teaching her particulars about IRMS use at Carnegie. We thank Bill Jamieson for drafting

774 the maps of site locations for Fig. 1. The acknowledgements in Gebru et al. (2009) and

775 Terwilliger et al. (2011) apply to this study as well. The work was funded by National

776 Science Foundation (USA) collaborative grants to Terwilliger (BCS-0551668) and Huang

777 (BCS-0551587).

778

## REFERENCES

- 779  
780
- 781 Adderley W. P. and Simpson I. A. (2005) Early-Norse home-field productivity in the Faroe  
782 Islands. *Human Ecology* **33**, 711-736.
- 783 Adderley, W. P. and Simpson, I. A. (2006) Soils and Palaeo-climate based evidence for  
784 irrigation requirements in Norse Greenland. *Journal of Archaeological Science* **33**,  
785 1666-1679.
- 786 Adderley W. P., Simpson I. A. and Davidson D. A. (2002) Colour description and  
787 quantification in mosaic images of soil thin sections. *Geoderma* **108**, 181-195.
- 788 Adderley W. P., Simpson I. A. and Davidson D. A. (2006) Historic landscape management: a  
789 validation of quantitative soil thin-section analyses. *Journal of Archaeological*  
790 *Science* **33**, 320-334.
- 791 Adderley W. P., Simpson I. A. and Vésteinsson O. (2008) Local-scale adaptations: a  
792 modeled assessment of soil, landscape, microclimatic, and management factors in  
793 Norse home-field productivities. *Geoarchaeology: An International Journal* **23**, 500-  
794 527.
- 795 Adderley W. P., Wilson C. A., Simpson I. A. and Davidson, D. A. (2010) Anthropogenic  
796 Features. In *Interpretation of Micromorphological Features of Soils and Regoliths*  
797 (eds. G. Stoops, V. Marcelino and F. Mees). Elsevier, Amsterdam, pp. 569-588.
- 798 Aimers J. (2011) Drought and the Maya: The story of the artefacts. *Nature* **479**, 44.
- 799 Association of Official Agricultural Chemists. (2000) *Official methods of AOAC International*,  
800 AOAC International, Gaithersburg, MD.
- 801 Bard, KA, Coltorti M., DiBlasi M. C., Dramis F. and Fattovich R. (2000) The environmental  
802 history of Tigray (Northern Ethiopia) in the Middle and Late Holocene: a preliminary  
803 outline. *African Archaeological Review* **17**, 65-86. Beck J., Sieber A. (2010) Is the  
804 spatial distribution of mankind's most basic economic traits determined by climate and  
805 soil alone? *PLoS ONE* **5**, e10416. doi:10.1371/journal.pone.0010416.
- 806 Bellwood P. (2005) *First farmers: the origins of agricultural societies*. Blackwell, Oxford.

807 Berakhi O., Brancaccio L., Calderoni.G., Coltorti M., Dramis F. and Umer M. (1998) The Mai  
808 Maiken sedimentary sequence: a reference point for the environmental evolution of  
809 the highlands of northern Ethiopia. *Geomorphology* **23**, 127-138.

810 Bossard, N., J. Jacob, C. Le Milbeau, E. Lallier-Vergès, V. J. Terwilliger, R. Boscardin. 2011.  
811 Variation in  $\delta D$  values of a single, species-specific molecular biomarker: a study of  
812 miliacin throughout a field of broomcorn millet (*Panicum miliaceum* L.). *Rapid*  
813 *Communications in Mass Spectrometry* **25**:2732-2740.

814 Büntgen U., Tegel W., Nicolussi K., McCormick M., Frank D., Trouet V., Kaplan J. O., Herzig  
815 F., Heussner K. U., Wanner H., Luterbacher J. and Esper J. (2011) 2500 years of  
816 European climate variability and human susceptibility. *Science* **331**, 578-582.

817 Butzer K. W. (1981) Rise and fall of Axum, Ethiopia: a geo-archaeological interpretation.  
818 *American Antiquity* **46**, 471-495.

819 Butzer K. W. (2005) Environmental history in the Mediterranean world: cross-disciplinary  
820 investigation of cause-and-effect for degradation and soil erosion. *Journal of*  
821 *Archaeological Science* **32**, 1773-1800.

822 CCSP. (2003) Vision for the Program and Highlights of the Scientific Strategic Plan: A  
823 Report by the Climate Change Science Program and the Subcommittee on Global  
824 Change Research, [http://www.climatechange.gov/Library/stratplan2003/vision/ccsp-](http://www.climatechange.gov/Library/stratplan2003/vision/ccsp-vision.pdf)  
825 [vision.pdf](http://www.climatechange.gov/Library/stratplan2003/vision/ccsp-vision.pdf).

826 Chalié F. and Gasse G. (2002) Late Glacial-Holocene diatom record of water chemistry and  
827 lake level change from the tropical East African Rift Lake Abiyata (Ethiopia).  
828 *Palaeogeography Palaeoclimatology and Palaeoecology* **187**, 259-283.

829 Chikaraishi Y. and Naraoka H. (2003) Compound specific  $\delta D$ — $\delta^{13}C$  analyses of *n*-alkanes  
830 extracted from terrestrial and aquatic plants. *Phytochemistry* **63**, 361-371.

831 Chikaraishi Y. and Naraoka H. (2007)  $\delta^{13}C$  and  $\delta D$  relationships among three *n*-alkyl  
832 compound classes (*n*-alkanoic acid, *n*-alkane and *n*-alkanol) of terrestrial higher  
833 plants. *Organic Geochemistry* **38**, 198-215. Chikaraishi Y., Naraoka H. and Poulson S.

834 R. (2004) Hydrogen and carbon isotopic fractionations of lipid biosynthesis among  
835 terrestrial (C<sub>3</sub>, C<sub>4</sub> and CAM) and aquatic plants. *Phytochemistry* **65**, 1369-1381.

836 Connah G. (2004) *Forgotten Africa: an Introduction to its Archaeology*. Routledge, London.

837 Cullen H. M., deMenocal P., Hemming S., Hemming G., Brown F. H., Guilderson T. and  
838 Sirocko R. (2000) Climate change and the collapse of the Akkadian empire: evidence  
839 from the deep sea. *Geology* **28**, 379-382.

840 Curtis M. C. (2009) Relating the Ancient Ona culture to the wider northern Horn: discerning  
841 patterns and problems in the archaeology of the First Millennium BC. *African*  
842 *Archaeological Review* **26**, 327-350.

843 D'Andrea A. C., Manzo A., Harrower J. J. and Hawkins A. L. (2008) The Pre-Aksumite and  
844 Aksumite settlement of NE Tigray, Ethiopia. *Journal of Field Archaeology* **33**, 151-  
845 176.

846 D'Andrea A. C., Richards M. P., Pavlish L. A., Wood S., Manzo A. and Wolde-Kiros H. S.  
847 (2011) Stable isotopic analysis of human and animal diets from two pre-  
848 Aksumite/Proto-Aksumite archaeological sites in northern Ethiopia. *Journal of*  
849 *Archaeological Science* **38**, 367-374.

850 Dansgaard W. (1964) Stable isotopes in precipitation. *Tellus* **5**, 461-469.

851 Dergachev V. A., Raspopov O. M., Damblon F., Jungner H. and Zaitseva G. I. (2007) Natural  
852 climate variability during The Holocene. *Radiocarbon* **49**, 837-854.

853 deMenocal P. B. (2001) Cultural responses to climate change during the Late Holocene.  
854 *Science* **292**, 667-673.

855 Diamond J. (2005) *Collapse: How Societies Choose To Fail Or Succeed*. Viking, New York.

856 DiBlasi M. C. (2005) Foreword. In *Changing Settlement Patterns in the Aksum-Yeha Region*  
857 *of Ethiopia: 700 BC – AD 850* (J. W. Michels) Cambridge Monographs in African  
858 Archaeology 64. BAR International Series 1446. Archaeopress Oxford, UK, pp. ix –  
859 xv. Disnar J. R., Guillet B., Keravis D., Di-Giovanni C. and Sebag D. (2003) Soil  
860 organic matter (SOM) characterization by Rock-Eval pyrolysis: scope and limitation.  
861 *Organic Geochemistry* **34**, 327-343.

862 Disnar J. R., Jacob J., Morched-Issa M., Lottier N. and Arnaud F. (2008) Assessment of peat  
863 quality by molecular and bulk geochemical analysis: application to the Holocene  
864 record of the Chautagne marsh (Haute Savoie, France). *Chemical Geology* **254**, 101-  
865 112.

866 Dramis F., Umer M., Calderoni G. and Haile M. (2003) Holocene climate phases from buried  
867 soils in Tigray (Northern Ethiopia): Comparison with lake level fluctuations in the  
868 Main Ethiopia Rifts. *Quaternary Research* **60**, 274-283.

869 Draper N. R. and Smith H. (1981) *Applied Regression Analysis (second edition)*. Wiley and  
870 Sons, New York. Drysdale R., Zanchetta G., Hellstrom J., Maas R., Fallick A., Pickett  
871 M., Cartwright I., and Piccini L. (2006) Late Holocene drought responsible for the  
872 collapse of Old World civilizations is recorded in an Italian cave flowstone. *Geology*  
873 **34**, 101-104.

874 Duiker W. J. and Spielvogel J. J. (2010) *World History (sixth edition)*. Wadsworth,  
875 Boston. Edwards K. J., Borthwick D., Cook G., Dugmore A. J., Mairs K.-A., Church M.,  
876 Simpson I. A. and Adderley W. P. (2005) A hypothesis-based approach to landscape  
877 change in Suðuroy, Faroe Islands. *Human Ecology* **33**, 621-649.

878 Eglinton G. and Hamilton R. J. (1967) Leaf epicuticular waxes. *Science* **156**, 1322-1335.

879 Ehret C. (2002) *The Civilizations of Africa*. University Press of Virginia, Charlottesville.

880 Emery K. F. and Thornton E. K. (2008) A regional perspective on biotic change during the  
881 Classic Maya occupation using zooarchaeological isotopic chemistry. *Quaternary*  
882 *International* **191**, 131-143.

883 Enquist B. J. and Enquist C. A. F. (2011) Long-term change within a Neotropical forest  
884 assessing differential functional and floristic responses to disturbance and drought.  
885 *Global Change Biology* **17**, 1408-1424.

886 Eshetu Z. (2002) Historical C3-C4 vegetation pattern on forested mountain slopes: its  
887 implication for ecological rehabilitation of degraded highlands of Ethiopia by  
888 afforestation. *Journal of Tropical Ecology* **18**, 743-758.

- 889 Eshetu Z. and Högberg P. (2000) Reconstruction of forest site history in Ethiopian  
890 highlands based on <sup>13</sup>C natural abundance of soils. *Ambio* **29**, 83-89.
- 891 Espitalié J., Deroo G. and Marquis F., (1985a) La pyrolyse Rock-Eval et ses applications :  
892 première partie. *Revue de l'Institut Français du Pétrole* **40**, 563-579.
- 893 Espitalié J., Deroo G. and Marquis F. (1985b) La pyrolyse Rock-Eval et ses applications :  
894 deuxième partie. *Revue de l'Institut Français du Pétrole* **40**, 755-784.
- 895 Estep M. F. and Hoering T. C. (1980) Biogeochemistry of the stable hydrogen isotopes.  
896 *Geochimica et Cosmochimica Acta* **44**, 1197-1206.
- 897 Estep M. F. and Hoering T. C. (1981) Stable hydrogen isotope fractionations during  
898 autotrophic and mixotrophic growth of microalgae. *Plant Physiology* **67**, 474-477.
- 899 Fattovich R. (1990) Remarks on the Pre-Aksumite Period in Northern Ethiopia. *Journal of*  
900 *Ethiopian Studies* **23**, 1-34.
- 901 Fattovich R. (2000) The cultural and historical context. In *The Aksum Archaeological Area: a*  
902 *Preliminary Assessment* (eds. R. Fattovich, K. A. Bard, L. Petrassi and V. Pisano).  
903 Working Paper 1, Istituto Universitario Orientale, Napoli, pp. 21-28.
- 904 Fattovich R. (2009) Reconsidering Yeha, c. 800 – 400 BC. *African Archaeological Review* **26**,  
905 275 – 290.
- 906 Feakins S. J. and Sessions A. L. (2010a) Controls on the D/H ratios of plant leaf waxes in an  
907 arid ecosystem. *Geochimica et Cosmochimica Acta* **74**, 2128-2141.
- 908 Feakins S. J. and Sessions A. L. (2010b) Crassulacean acid metabolism influences D/H  
909 ratio of leaf wax in succulent plants. *Organic Geochemistry* **41**, 1269-1276.
- 910 Filipelli G. M., Souch C., Horn S. P. and Newkirk D. (2010) The pre-Columbian footprint on  
911 terrestrial nutrient cycling in Costa Rica: insights from phosphorus in a lake sediment  
912 record. *Journal of Paleolimnology* **43**, 843-856.
- 913 French C., Sulas F., Madella M. (2009) New geoarchaeological investigations of the valley  
914 systems in the Aksum area of northern Ethiopia. *Catena* **78**, 218-233.

915 Friis I. (1992) *Forests and forest trees of north east Tropical Africa: their natural habitats and*  
916 *Distribution patterns in Ethiopia, Djibouti and Somalia*. London:Royal Botanic  
917 Gardens, Kew Bulletin Additional series xv, HMSO.

918 Galang M. A., Markewitz D. and Morris L. A. (2010) Soil phosphorus transformations under  
919 forest burning and laboratory heat treatments. *Geoderma* **155**, 401-408.

920 Gani N. D., Gani M. R. and Abdelsalam M. G. (2007) Blue Nile incision on the Ethiopian  
921 Plateau: pulsed plateau growth, Pliocene uplift, and hominin evolution. *GSA Today*  
922 **17**, 4-11.

923 Garcin Y, Schwab V. F., Gleixner G., Kahmen A., Todou G., Séné O., Onana J.-M.,  
924 Achoundong G. and Sachse D.(2012) Hydrogen isotope ratios of lacustrine  
925 sedimentary *n*-alkanes as proxies of tropical African hydrology: Insights from a  
926 calibration transect across Cameroon. *Geochimica et Cosmochimica Acta* **79**, 106-  
927 126.

928 Gasse F. (2000) Hydrological changes in the African tropics since the Last Glacial Maximum.  
929 *Quaternary Science Reviews* **19**, 189-211.

930 Gat J. R. (1980) The isotopes of hydrogen and oxygen in precipitation. In *Handbook of*  
931 *Environmental Isotope Geochemistry* **1**, 21-47.

932 Gebru T., Eshetu Z., Huang Y., Woldemariam T., Strong N., Umer M., DiBlasi M. and  
933 Terwilliger V. J. (2009) Holocene palaeovegetation of the Tigray Plateau in northern  
934 Ethiopia from charcoal and stable organic carbon isotopic analyses of gully  
935 sediments. *Palaeogeography, Palaeoclimatology, and Palaeoecology* **282**, 67-80.

936 Gelfand M. J., Raver J. L., Nishii L., Leslie L. M., Lun J., Lim B. C., Duan L., Almaliach A.,  
937 Ang S., Arnadottir J., Aycan Z., Boehnke K., Boski P., Cabecinhas R., Chan D.,  
938 Chhokar J., D'Amato A., Ferrer M., Fischlmayr I. C., Fischer R., Fülöp M., Georgas J.,  
939 Kashima E. S., Kashima Y., Kim K., Lempereur A., Marquez P., Othman R., Overlaet  
940 B., Panagiotopoulou P., Peltzer K., Perez-Florizno L. R., Ponomarenko L., Realo A.,  
941 Schei V., Schmitt M., Smith P. B., Soomro N., Szabo E., Taveesin N., Toyama M.,

942 Van de Vliert E., Vohra N., Ward C. and Yamaguchi S. (2011) Differences Between  
943 Tight and Loose Cultures: A 33-Nation Study. *Science* **332**, 1100–1104.

944 Giorgi F., Diffenbaugh N. S., Gao X. J., Coppola E., Dash S. K., Frumento O., Rauscher S.  
945 A., Remedio A., Sanda I. S., Steiner A., Sylla B. and Zekey A. S. (2008) The regional  
946 climate change hyper-matrix framework. *EOS* **89**, 445-446.

947 Harrower MJ, McCorrison J and D'Andrea AC. (2010) General/specific, local/global:  
948 comparing the beginnings of agriculture in the Horn of Africa (Ethiopia/Eritrea) and  
949 Southwest Arabia (Yemen). *American Antiquity* **75**, 452-472.

950 Hassan R. (1997) Nile floods and political disorder in early Egypt. In *Third millennium B.C.*  
951 *Climate Change and Old World Collapse* (ed. H. N. Dalfes). Springer, Berlin, **49**, pp.  
952 1-23.

953 Hatch M. D. (1978) Regulation of enzymes in C<sub>4</sub> photosynthesis. *Current Topics in Cellular*  
954 *Regulation* **14**, 1-27.

955 Haug G. H., Günther D., Peterson L. C., Sigman D. M., Hughen K. A. and Aeschlimann B.  
956 (2003) Climate and the collapse of Maya civilization. *Science* **299**, 1731-1735.

957 Hodell D. (2011) Drought and the Maya: Maya megadrought? *Nature* **479**, 44.

958 Hou J., D'Andrea W. J. and Y. Huang. (2008) Can sedimentary leaf waxes record D/H  
959 ratios of continental precipitation? Field, model, and experimental assessments.  
960 *Geochimica et Cosmochimica Acta* **72**, 3503-3517.

961 IPCC-Intergovernmental Panel on Climate Change. (2007) Climate change 2007: the  
962 physical science basis. Contribution of Working Group I to the Fourth Assessment  
963 Report of the IPCC, Geneva. (eds. S. Solomon, D. Qin, M. Manning, Z. Chen, M.  
964 Marquis, K. B. Avery, M. Tignor and H. L. Miller, eds.) Cambridge University Press,  
965 Cambridge, UK. [http://www.ipcc.ch/publications\\_and\\_data/ar4/wg1/en/contents.html](http://www.ipcc.ch/publications_and_data/ar4/wg1/en/contents.html) .

966 Jackson P. C., Meinzer F. C., Bustamante M., Goldstein G., Franco A., Rundel P. W., Caldas  
967 L., Iglar E. and Causin F. (1999) Partitioning of soil water among tree species in a  
968 Brazilian Cerrado ecosystem. *Tree Physiology* **19**, 717-724.

969 Jones D., Briffa K. R., Osborn T. J., Lough J. M., van Ommen T. D., Vinther B. M.,  
970 Luterbacher J., Wahl E. R., Zwiars F. W., Mann M. E., Schmidt G. A., Ammann C. M.,  
971 Buckley B. M., Cobb K. M., Esper J., Goosse H., Graham N., Jansen E., Kiefer T.,  
972 Kull C., Küttel M., Mosley-Thompson E., Overpeck J. T., Riedwyl N., Schulz M.,  
973 Tudhope A. W., Villalba R., Wanner H., Wolff E. and Xoplaki E. (2009) High-  
974 resolution palaeoclimatology of the last millennium: a review of current status and  
975 future prospects. *The Holocene* **19**, 3-49.

976 Kolattukudy P. E. (1970) Biosynthesis of cuticular lipids. *Annual Review of Plant Physiology*  
977 **21**, 163-192.

978 Krull E., Sachse D., Mügler I, Thiele A., Gleixner G. (2006) Compound-specific  $\delta^{13}\text{C}$  and  $\delta^2\text{H}$   
979 analyses of plant and soil organic matter: A preliminary assessment of the effects of  
980 vegetation change on ecosystem hydrology. *Soil Biology & Biochemistry* **38**, 3211–  
981 3221.

982 Lafargue E., Marquis F. and Pillot D. (1998) Rock-Eval 6 applications in hydrocarbon  
983 exploration, production, and soil contamination studies. *Revue de l'Institut Français*  
984 *du Pétrole* **53**, 421-437.

985 Machado M. J., Perez-Gonzalez, A. and Benito G. (1998) Paleoenvironmental changes  
986 during the last 4000 years in the Tigray, northern Ethiopia. *Quaternary Research* **49**,  
987 312-321.

988 Marshall M. H., Lamb H. F., Davies S. J., Leng M. J., Kubsa Z., Umer M. and Bryant, C.,  
989 (2009) Climatic change in northern Ethiopia during the past 17,000 years: a diatom  
990 and stable isotope record from Lake Ashenge. *Palaeogeography, Palaeoclimatology,*  
991 *Palaeoecology* **279**, 114-17.

992 Marshall M. H., Lamb H. F., Huws D., Davies S. J., Bates R., Bloemendal J., Boyle J. Leng  
993 M. J., Umer M. and Bryant C. (2011) Late Pleistocene and Holocene drought events  
994 at Lake Tana, the source of the Blue Nile. *Global and Planetary Change* **78**, 147-161.

995 Mastrandrea M.D. and Schneider S.H. (2010). *Preparing for Climate Change*. MIT Press,  
996 Cambridge, MA.

997 McGovern T. H. (1994) Management for Extinction in Norse Greenland. *In Historical*  
998 *Ecology: Cultural Knowledge and Changing Landscapes* (ed. C. Crumley). Santa Fe  
999 School of American Research Monograph, pp. 127-154.

1000 McInerney F. A., Helliker B. R. and Freeman K. H. (2011) Hydrogen isotope ratios of leaf  
1001 wax *n*-alkanes in grasses are insensitive to transpiration. *Geochimica et*  
1002 *Cosmochimica Acta* **75**, 541-554.

1003 Munsell Soil Color Charts. (1994) Macbeth Division of Kollmorgen Instruments Corporation,  
1004 New Windsor, NY.

1005 Murphy C. P. (1984) The overestimation of clay and the underestimation of pores in soil thin-  
1006 sections. *Journal of Soil Science* **35**, 481-495.

1007 National Meteorological Agency of Ethiopia. (1998-2006) Available through  
1008 [http://www.ethiomet.gov.et/stations/regional\\_information/1](http://www.ethiomet.gov.et/stations/regional_information/1).

1009 Niedermeyer E. R., Schefuss E., Sessions A. L., Mulitza S., Mollenhauer G., Schulz M. and  
1010 Wefer G. (2010) Orbital- and millennial-scale changes in the hydrologic cycle and  
1011 vegetation in the western African Sahel: insights from individual plant wax  $\delta D$  and  
1012  $\delta^{13}C$ . *Quaternary Science Reviews* **29**, 2996–3005.

1013 Nobel, P.S. (1999) *Physicochemical and Environmental Plant Physiology*, 2nd edition.  
1014 Academic Press, San Diego.

1015 Nyssen J., Poesen J., Moeyersons J., Deckers J., Haile M. and Lang A., (2004) Human  
1016 impact on the environment in the Ethiopian and Eritrean highlands-a state of the art.  
1017 *Earth Science Reviews* **64**, 273-320.

1018 Oosterbaan R. J. (no date) <http://www.waterlog.info/segreg.htm>.

1019 Oosterbaan R. J., Sharma D. P., Singh K. N. and Rao K. V. G. K. (1990) Crop production  
1020 and soil salinity: evaluation of field data from India by segmented linear regression  
1021 with breakpoint. Session V, Proceedings of the Symposium on Land Drainage for  
1022 Salinity Control in Arid and Semi-Arid Regions, Cairo, February 1990 **3**, 373-383.

- 1023 Patterson W. P., Dietrich K. A., Holmden C. and Andrews J. T. (2010) Two millennia of  
1024 North Atlantic seasonality and implications for Norse colonies. *Proceedings of the*  
1025 *National Academy of Sciences* **107**, 5306-5310.
- 1026 Phillipson D. W. (1998) *Ancient Ethiopia, Aksum: its Antecedents and Successors*. British  
1027 Museum Press, London.
- 1028 Polissar P. J., Freeman K. H. (2010) Effects of aridity and vegetation on plant-wax  $\delta D$  in  
1029 modern lake sediments. *Geochimica et Cosmochimica Acta* **74**, 5785-5797.
- 1030 Reimer P. J., Baillie M. G. L., Bard E., Bayliss A., Beck J. W., Bertrand C. J. H., Blackwell P.  
1031 G., Buck C. E., Burr G. S., Cutler K.B., Damon P.E., Edwards R.L., Fairbanks R.G.,  
1032 Friedrich M., Guilderson T. P., Hogg A., Hughen K. A., Kromer B., McCormac G.,  
1033 Manning S., Ramsey C. B., Reimer R. W., Remmele S., Southon J. R., Stuiver M.,  
1034 Talamo S., Taylor F. W., van der Plicht J., Weyhenmeyer C. E. (2004) INTCAL04  
1035 terrestrial radiocarbon age calibration, 0 - 26 cal kyr BP. *Radiocarbon* **46**, 1029–1058.
- 1036 Rein G., Cleaver N., Ashton C., Pironi P., and Torero J. (2008) The severity of smouldering  
1037 peat fires and damage to the forest soil. *Catena* **74**, 304-309.
- 1038 Resende J. C. F., Markewitz D., Klink C. A., Bustamante M. M. da C. and Davidson E. A.  
1039 (2011) Phosphorus cycling in a small watershed in the Brazilian Cerrado: impacts of  
1040 frequent burning. *Biogeochemistry* **105**, 105-118.
- 1041 Rhoades J. D. and Corwin D. L. (1993) Electrical conductivity methods for measuring and  
1042 mapping soil salinity. *Advances in Agronomy* **49**, 201–251.
- 1043 Richardson C. J. (1985) Mechanisms controlling phosphorous retention capacity in  
1044 freshwater wetlands. *Science* **228**, 1424-1427.
- 1045 Risi C., Bony S. and Vimeux F. (2008) Influence of convective processes on the isotopic  
1046 composition ( $\delta^{18}O$  and  $\delta D$  of precipitation and water vapor in the tropics: 2. Physical  
1047 interpretation of the amount effect. *Journal of Geophysical Research* **113**,  
1048 doi:10.1029/2008JD009943.

1049 Robin C. and de Maigret A. (1998) Le Grand Temple de Yéha (Tigray, Ethiopie), après la  
1050 première campagne de fouilles de la Mission française (1998). *Comptes-rendus des*  
1051 *Séances de l'Académie des Inscriptions et Belles-Lettres* **142**, 737-798.

1052 Ruben S., Randall M., Kamen M. D. and Hyde J. L. (1941) Heavy oxygen ( $^{18}\text{O}$ ) as tracer in  
1053 the study of photosynthesis. *Journal of the American Chemical Society* **63**, 877-878.

1054 Sachse D., Radke J., and Gleixner G. (2004) Hydrogen isotope ratios of recent lacustrine  
1055 sedimentary *n*-alkanes. *Geochimica et Cosmochimica Acta* **68**, 4877-4889.

1056 Sachse D., Radke J., and Gleixner G. (2006)  $\delta\text{D}$  values of individual *n*-alkanes from  
1057 terrestrial plants along a climatic gradient—Implications for the sedimentary  
1058 biomarker record. *Organic Geochemistry* **37**, 469-483.

1059 Sachse D., Billault I., Bowen G. J., Chikaraishi Y., Dawson T. E., Feakins S. J., Freeman K.  
1060 H., Magill C. R., McInerney F. A., van der Meer B. T. J., Polissar P., Robins R. J.,  
1061 Sachs J. P., Schmidt H.-L., Sessions A. L., White J. W. C., West J. B. and Kahmen A.  
1062 (2012) Molecular paleohydrology: interpreting the hydrogen-isotopic composition of  
1063 lipid biomarkers from photosynthesizing organisms. *Annual Review of Earth and*  
1064 *Planetary Sciences* **40**, 221-249.

1065 Schoeneberger P. J., Wysocki D. A., Benham E. C. and Broderson, W. D. (eds), 2002.  
1066 *Field book for describing and sampling soils*, Version 2.0. Natural Resources  
1067 Conservation Service, National Soil Survey Center, Lincoln, NE.

1068 Sessions A. L., Burgoyne T. W., Schimmelmann A., and Hayes J. M. (1999) Fractionation of  
1069 hydrogen isotopes in lipid biosynthesis. *Organic Geochemistry* **30**, 1193-1200.

1070 Simpson I. A., Adderley W. P., Guðmundsson G., Hallsdóttir, Sigurgeirsson M. Á. and  
1071 Snæsdóttir M. (2002) Soil limitations to agrarian land production in premodern  
1072 Iceland. *Human Ecology* **30**, 423-443.

1073 Simpson I. A., Vesteinsson O., Adderley W. P. and McGovern T. H. (2003) Fuel resource  
1074 utilisation in landscapes of settlement. *Journal of Archaeological Science* **30**, 1401-  
1075 1420.

1076

- 1077 Smith F. A. and Freeman K. H. (2006) Influence of physiology and climate on  $\delta D$  of leaf wax  
1078 *n*-alkanes from C<sub>3</sub> and C<sub>4</sub> grasses. *Geochimica et Cosmochimica Acta* **70**, 1172-  
1079 1187.
- 1080 Soil Survey Staff., (1995) *Soil Survey Laboratory Information Manual*. USDA, Natural  
1081 Resources Conservation Service, Soil Survey Investigations Report No. 45, Version  
1082 1.0. National Soil Survey Center. Lincoln, NE.
- 1083 Sokal R. R. and Rohlf F. J. (1995) *Biometry: the Principles and Practice of Statistics in*  
1084 *Biological Research (third edition)*. Freeman, New York.
- 1085 Stager J. C. and Mayewski P. A. (1997) Abrupt early to mid-Holocene climatic transition  
1086 registered at the equator and the poles. *Science* **276**, 1834–1836.
- 1087 Sternberg L. S. L. (1989) Oxygen and hydrogen isotope ratios in plant cellulose: mechanisms  
1088 and applications. In *Stable Isotopes in Ecological Research* (eds. P. W. Rundel, J. R.  
1089 Ehleringer and K. A. Nagy) Springer , New York, pp. 124–141.
- 1090 Sternberg L., DeNiro M. J. and Agie H. (1984) Stable hydrogen isotope ratios of saponifiable  
1091 lipids and cellulose nitrate from CAM, C<sub>3</sub> and C<sub>4</sub> plants. *Phytochemistry* **23**, 2475-  
1092 2477.
- 1093 Stowe L. G. and Teeri J. A. (1978) The geographic distribution of C<sub>4</sub> species of the  
1094 dicotyledonae in relation to climate. *American Naturalist* **112**, 609-623.
- 1095 Stuiver M. and Reimer, P. (1986-2005) CALIB 5.0.2. <http://calib.qub.ac.uk/calib>.
- 1096 Stuiver M. and Reimer P. (1993) Extended <sup>14</sup>C data base and revised calib 3.0 <sup>14</sup>C age  
1097 calibration program. *Radiocarbon* **35**, 215-230.
- 1098 Sulas F. (2010) Environmental and cultural interplay in highland Ethiopia: geoarchaeology at  
1099 Aksum. Ph. D. thesis, University of Cambridge, Department of Archaeology,  
1100 Cambridge, UK.
- 1101 Teeri J. (1988) Interaction of temperature and other environmental variables influencing  
1102 plant distribution. *Symposia of the Society for Experimental Biology* **42**, 77–89.
- 1103 Telford J. J., Heegaard E., and Birks H. M. B. (2004) The intercept is a poor estimate of a  
1104 calibrated radiocarbon age. *The Holocene* **14**, 296–298.

- 1105 Terwilliger V. J., Eshetu Z., Alexandre M., Huang Y., Umer M. and Gebru T. (2011) Local  
1106 variation in climate and land use during the time of the major kingdoms of the Tigray  
1107 Plateau of Ethiopia and Eritrea. *Catena* **85**, 130-143.
- 1108 Terwilliger V.J., Eshetu Z., Colman A., Bekele T., Gezahgne A. and Fogel M.L. 2008.  
1109 Reconstructing palaeoenvironment from  $\delta^{13}\text{C}$  and  $\delta^{15}\text{N}$  values of soil organic matter:  
1110 a calibration from arid and wetter elevation transects in Ethiopia. *Geoderma* **147**,  
1111 197-210.
- 1112 Thomson D. J. (1990) Time series analysis of Holocene climate data. *Philosophical*  
1113 *Transactions of the Royal Society of London. Series A, Mathematical and Physical*  
1114 *Sciences* **330**, 601-616.
- 1115 Tierney J., Lewis S. C., Cook B. I., LeGrande A. N. and Schmidt G. A. (2011) Model, proxy  
1116 and isotopic perspectives on the East African Humid Period. *Earth and Planetary*  
1117 *Science Letters* **307**, 103-112.
- 1118 Trouve C., Mariotti A., Schwarz D. and Geuillet, B. (1994) Soil organic carbon dynamics  
1119 under Eucalyptus and Pinus planted on savanna in the Congo. *Soil Biology and*  
1120 *Biochemistry* **26**, 287-295.
- 1121 Turchin P. (2008) Arise 'cliodynamics'. *Nature* **454**, 34-35.
- 1122 Vimeux F., Masson V., Jouzel J., Stievenard M. and Petit J. R. (1999) Glacial-interglacial  
1123 changes in ocean surface conditions in the southern hemisphere. *Nature* **398**, 410-  
1124 413.
- 1125 Weiss H. and Bradley S. (2001) What drives societal collapse? *Science* **291**, 609-610.
- 1126 Weiss H., Courty M. A., Wetterstrom W., Guichard F., Senior L., Meadow T., and Curnow A.  
1127 (1993). The genesis and collapse of third millennium North Mesopotamian  
1128 civilization. *Science* **261**, 995-1004.
- 1129 Whalley W. R., Riseley B., Leeds-Harrison P. B., Bird N. R. A., Leech P. K. and Adderley W.  
1130 P. (2005) Structural differences between bulk and rhizosphere soil. *European*  
1131 *Journal of Soil Science* **56**, 353-360.

- 1132 Worden J., Noone D. and Bowman K. (2007) Importance of rain evaporation and continental  
1133 convection in the tropical water cycle. *Nature* **445**, 528-532.
- 1134 Yakir, D. (1992) Variations in the natural abundance of oxygen-18 and deuterium in plant  
1135 carbohydrates. *Plant, Cell and Environment* **15**, 1005-1020.
- 1136 Yurtsever Y. (1975) Worldwide survey of stable isotopes in precipitation. *Report Section*  
1137 *Isotope Hydrology*. International Atomic Energy Association, Vienna.
- 1138 Zhang X., Gillespie A. L. and Sessions A. (2009) Large D/H variations in bacterial lipids  
1139 reflect central metabolic pathways. *Proceedings of the National Academy of*  
1140 *Sciences* **106**, 12580-12586.
- 1141

1142 **Figure legends.**

1143

1144 **Figure 1.** Locations of study sites and sequences.

1145

1146 **Figure 2.** Lithology and salinity related characteristics of study sections at Adi Kolen (AKIII),  
1147 Adigrat (ATI), and Mai Maikden (MMII). Closed circles indicate where charcoaled wood was  
1148 found and dates are those used to estimate age-depth relationships (see text). Open circles  
1149 indicate samples where charcoal was not found. The arrows in AKIII and MMII point to  
1150 unconformities with large associated hiati in time. Interpolated dates used to estimate rate  
1151 changes indicated by lithology are marked with an X. Rjck fragment modifiers accompanying  
1152 texture names follow the USDA classification where in a total soil sample,  $15\% \leq$  gravelly or  
1153 cobbly  $< 35\%$  and  $60\% \leq$  extremely gravelly or cobbly (Soil Survey Staff, 1995). The two  
1154 columns per section of soil physical properties are modified from Gebru et al., (2009) and  
1155 Terwilliger et al. (2011).

1156

1157 **Figure 3.**  $\delta D_{n-C26}$  values (‰ VSMOW),  $\delta^{13}C$  of bulk organic matter (‰ PDB), and estimated  
1158  $\%C_4$  plant of total plant-derived C in all three sections. Closed circles connected by solid  
1159 lines are for the section at Adi Kolan (AKIII), open circles connected by long dashed lines are  
1160 for the Mai Maikden section MMII, and x symbols connected by short dashed lines are for the  
1161 Adigrat section ATI. The plots of  $\delta^{13}C$  are modified from Gebru et al. (2009) and Terwilliger  
1162 et al. (2011).

1163

1164 **Figure 4.** Trends in  $\delta D_{n-C26}$  and bulk organic  $\delta^{13}C$  values (A) with accompanying non-isotopic  
1165 factors in MMII.  $\%C_4$  is estimated  $\%C_4$  plant of total plant-derived C, TOC is total organic  
1166 carbon and Identified charcoal % is the % of all identifiable charcoaled wood fragments in a  
1167 sample that were from the indicated vegetation type (A). HI and OI are hydrogen and  
1168 oxygen indices from Rock-Eval pyrolysis, Total P is phosphorus content, and Char is charred  
1169 matter (B). Open circles indicate data used for correlation analyses with other factors. In

1170 factors where these values were only a subset of the all the data analyzed ( $\delta^{13}\text{C}$  and %TOC),  
1171 the remaining data are shown as closed black symbols. Short-dashed, dark gray lines  
1172 indicate significant, long-term trends in all values of a factor over time. In the factors where  
1173 data subsets were used in segmented regression analyses (not identified charcoal%); short  
1174 dashed black lines indicate the long-term trends of the data subsets. The plots of  $\delta^{13}\text{C}$ ,  
1175 %TOC, and Identified charcoal % are modified from Gebru et al. (2009).

1176

1177 **Figure 5.** Trends in  $\delta\text{D}_{n\text{-C}26}$  and bulk organic  $\delta^{13}\text{C}$  values, and accompanying non-isotopic  
1178 factors in AKIII. See Fig. 4 for explanation of lines and labels. The plots of  $\delta^{13}\text{C}$ , %TOC, nd  
1179 Identified charcoal % are modified from Gebru et al. (2009) and Terwilliger et al. (2011).

1180

1181 **Figure 6.** Trends in  $\delta\text{D}_{n\text{-C}26}$  and bulk organic  $\delta^{13}\text{C}$  values with accompanying non-isotopic  
1182 factors in ATI. See Fig. 3 for explanation of lines and labels. The plots of  $\delta^{13}\text{C}$ , %TOC, nd  
1183 Identified charcoal % are modified from Gebru et al. (2009) and Terwilliger et al. (2011).

## Appendix A

Dry structure, structure grade, consistence, and color data for study sections presented in this paper. The structural and consistence descriptions were developed from the guidelines in Schoeneberger et al. (2002). Color descriptions, hue, value, and chroma were determined from Munsell Soil Color Charts (1994). The data from AKIII and ATI can also be found in the Supplemental materials of Terwilliger et al., (2011).

Section	Depth (cm)	Structure	Grade	Consistence	Color	Hue Value/Chroma
AKIII	0	granular	structureless-weak	soft	yellowish brown	10YR 5/8
	30	granular	weak	soft	yellowish brown	10YR 5/6
	60	granular-subangular blocky	weak-moderate	slightly hard	yellowish brown	10YR 5/4
	100	granular-subangular blocky	weak-moderate	slightly hard	dark yellowish brown	10YR 4/3
	130	granular-subangular blocky	weak-moderate	slightly hard	dark yellowish brown	10YR 4/3
	160	granular-subangular blocky	weak-moderate	slightly hard	dark yellowish brown	10YR 4/3
	190	granular-subangular blocky	weak-moderate	soft-slightly hard	dark yellowish brown	10YR 4/3
	220	subangular blocky	moderate	moderately hard	dark yellowish brown	10YR 4/3
	270	granular-subangular blocky	weak-moderate	slightly-moderately hard	dark yellowish brown	10YR 4/3
	295	subangular blocky	moderate-strong	hard	dark brown	7.5YR 3/2
	305	subangular blocky	moderate	moderately hard	dark brown	7.5YR 3/2
	320	subangular blocky	moderate-strong	hard	dark brown	7.5YR 3/2
	360	granular-subangular blocky	moderate	moderately hard	very dark brown	7.5YR 2.5/2
	440	subangular blocky	moderate-strong	hard	dark brown	7.5YR 3/2
	470	granular-subangular blocky	moderate	hard	yellowish brown	10YR 5/4

	490	granular-subangular blocky	weak-moderate	slightly-moderately hard	brownish yellow	10YR 6/6
	510	granular-subangular blocky	weak-moderate	soft-slightly hard	light yellowish brown	10YR 6/4
	540	subangular blocky	moderate-strong	hard	dark grayish brown	10YR 4/2
	560	granular-subangular blocky	weak-moderate	slightly-moderately hard	yellowish brown	10YR 5/4
	580	granular-subangular blocky	weak	soft	brownish yellow	10YR 6/6
	620	granular	weak	loose-soft	brownish yellow	10YR 6/8
	660	granular	weak	loose-soft	brownish yellow	10YR 6/8
MM II	0	granular	structureless	loose-soft	dark yellowish brown	10YR 4/4
	10	granular-subangular blocky	structureless-weak	loose-soft	yellowish brown	10YR 5/4
	20	subangular blocky	moderate	moderately hard	yellowish brown	10YR 5/4
	30	subangular blocky	weak	slightly hard	dark grayish brown	10YR 4/2
	35	subangular blocky	weak	slightly hard	grayish brown	10YR 5/2
	45	subangular blocky	weak	slightly hard	grayish brown	10YR 5/2
	60	sub-angular blocky	weak	slightly-moderately hard	light gray	10YR 7/2
	90	granular-subangular blocky	structureless-weak	loose-soft	light gray	10YR 7/2
	100	subangular blocky	weak	moderately hard	greenish gray	gley 4/1 10Y
	110	subangular blocky	weak	slightly hard	dark greenish gray	gley 3/1 10Y
	115	subangular blocky	weak	slightly hard	pale red	2.5YR 7/2
	130	subangular blocky	weak	slightly hard	reddish gray	2.5YR 5/1
	155	subangular blocky	weak	slightly hard	light greenish gray	gley 7/1 10Y
	170	angular blocky	weak	moderately hard	gray	gley 5/N

180	subangular blocky	weak	slightly hard	greenish gray	gley 5/1 10Y
190	subangular blocky	weak	slightly hard	greenish gray	gley 6/1 10Y
200	subangular blocky	weak	slightly hard	light greenish gray	gley 7/1 10Y
220	subangular blocky	weak	slightly hard	light gray	5Y 7/2
230	subangular blocky	weak	moderately hard	light gray	5Y 7/2
245	angular blocky	weak	slightly hard	greenish gray	gley 6/1 10Y
250	subangular blocky	weak	slightly hard	light gray	5Y 7/2
280	subangular blocky	weak	soft	greenish gray	gley 5/1 5GY
300	subangular blocky	weak	slightly hard	light gray	10R 7/1
310	subangular blocky	weak	moderately hard	pale red	10R 7/2
320	angular blocky	weak	slightly hard	dark greenish gray	gley 4/1 10Y
330	subangular blocky	weak	moderately hard	dark greenish gray	gley 3/1 10Y
340	granular	structureless-weak	loose-soft	strong brown	7.5YR 5/8
355	angular blocky	weak	slightly hard	very dark gray	gley 3/N
360	granular	structureless-weak	loose-soft	light gray	10YR 7/1
370	subangular blocky	weak	moderately hard	dark greenish gray	gley 3/1 10Y
380	angular blocky	weak	slightly hard	very dark gray	gley 3/N
386	granular	structureless-weak	loose-soft	light gray	10YR 7/1
390	subangular blocky	weak	soft	gray	10YR 6/1
400	angular blocky	weak	slightly hard	very dark gray	gley 3/N
414	subangular blocky	weak	soft	gray	10YR 6/1
425	granular	structureless-weak	loose-soft	light gray	5YR 7/1
470	subangular blocky	weak	moderately hard	pinkish gray	5YR 7/2
480	granular	structureless-weak	loose-soft	light gray	10YR 7/1

	510	subangular blocky	weak	slightly hard	pinkish gray	5YR 7/2
	530	subangular blocky	weak	slightly hard	light gray	5YR 7/1
	540	subangular blocky	weak	moderately hard	pinkish gray	5YR 7/2
	550	angular blocky	weak	slightly hard	very dark gray	gley 3/N
	560	granular	structureless	loose	pinkish gray	7.5YR 7/2
	580	subangular blocky	weak	slightly hard	light gray	5YR 7/1
	595	angular blocky	weak	hard	gray	5YR 5/1
	640	angular blocky	weak	slightly hard	very dark gray	gley 3/N
ATI	0	granular- subangular blocky	weak- moderate	loose-soft	yellowish brown	10YR 5/6
	100	granular- subangular blocky	moderate	slightly hard	dark yellowish brown	10YR 4/4
	130	granular- subangular blocky	weak- moderate	slightly hard	dark yellowish brown	10YR 4/4
	180	granular- subangular blocky	weak- moderate	slightly- moderately hard	dark yellowish brown	10YR 4/6
	210	subangular blocky	moderate	moderately hard	yellowish brown	10yr 5/4
	250	granular- subangular blocky	weak- moderate	slightly hard	yellowish brown	10YR 5/6
	310	single grain- granular	structureless- weak	slightly- moderately hard	light yellowish brown	10YR 6/4
	320	granular- subangular blocky	weak	slightly hard	light yellowish brown	10YR 6/4
	360	single grain- granular	structureless- weak	loose	pale brown	10YR 6/3
	370	granular- subangular blocky	weak	soft	light yellowish brown	10YR 6/4
	430	granular- subangular blocky	structureless- weak	soft	light yellowish brown	10YR 6/4
	470	single grain	structureless	loose	brownish yellow	10YR 6/6

Table 1. Radiocarbon and calibrated calendar dates of sections at Adi Kolan, Mai Maikden, and Adigrat.

Site	Section	Depth (cm)	UCIAMS #	Radiocarbon age ( $^{14}\text{C}$ yr BP)	Calibrated age range (cal yr BP) (2 $\sigma$ , 95.4%)	Relative area under distribution	Median age from probability distribution (cal yr BP)
Adi Kolan	AKIII	30	53894	105 $\pm$ 15	27–47, 55–140, 221–259	0.119, 0.595, 0.285	113
		100	36088	855 $\pm$ 15	788–731	1.000	759
		220	36089	2345 $\pm$ 15	2356–2340	1.000	2349
		305	36090	2420 $\pm$ 20	2491–2354, 2607–2603, 2677–2642	0.899, 0.005, 0.096	2429
		360	53897	3890 $\pm$ 15 <sup>a</sup>	4250–4274, 4284–4413	0.075, 0.925	4343
		540	36091	3600 $\pm$ 15	3931–3847, 3970–3942	0.817, 0.183	3903
		620	53895	12035 $\pm$ 30	13793–1399030	1.000	13887
		660	36109	11735 $\pm$ 25	13701–13597	1.000	13597
Mai Maikden	MMII	30	36111	130 $\pm$ 15	1–3, 41–12, 148–60, 199–187, 233–211, 269–241	0.002, 0.168, 0.519, 0.024, 0.118, 0.169	112
		320	36124	5640 $\pm$ 100 <sup>b</sup>	6228–6223, 6664–6277	0.002, 0.998	6437
		385	36100	6130 $\pm$ 15	7029–6946, 7069–7051, 7084–7078, 7156–7098	0.663, 0.029, 0.006, 0.302	7005
		470	36101	6625 $\pm$ 20	7568–7469	1.000	7519
		575	36102	7055 $\pm$ 20	7941–7844	1.000	7892
Adigrat	ATI	000	53896	395 $\pm$ 15	336–348, 454–505	0.06, 0.94	485
		100	36092	1345 $\pm$ 15	1298–1269	1.000	1287
		210	36110	1045 $\pm$ 15 <sup>a</sup>	969–929	1.000	949
		360	36093	2460 $\pm$ 15	2414–2364, 2545–2433, 2572–2561, 2617–2584, 2701–2635	0.084, 0.375, 0.017, 0.144, 0.381	2591
		470	36094	2680 $\pm$ 15	2794–2752, 2843–2823	0.926, 0.074	2773

All analyses were performed at the University of California Irvine Keck Carbon Cycle Accelerator Mass Spectrometry lab, Earth System Science Department (UCIAMS). Size-dependent sample preparation backgrounds were subtracted based on measurements of  $^{14}\text{C}$ -free wood. Radiocarbon ages were corrected for isotopic fractionation according to the conventions of Stuiver and Polach (1977), with  $\delta^{13}\text{C}$  values measured on prepared graphite using the AMS. These can differ from  $\delta^{13}\text{C}$  of the original material, if fractionation occurred during sample graphitization or the AMS measurement, and are not shown. All of the dated samples were charcoalized wood. Radiocarbon ages were calibrated using CALIB v5.0.2 (Stuiver and Reimer, 1993) using the INTCAL04.14c dataset (Reimer et al. 2004). All samples were charcoal. This table shows data from Table 2 of Gebru et al. (2009) and Table 1 of Terwilliger et al (2011).

<sup>a</sup> Samples suggest redeposition.

<sup>b</sup>The large uncertainty is due to the very small sample size (0.025 mg).

Table 2.  $\delta D$  values of land-plant derived fatty acids, date matched bulk organic  $\delta^{13}C$  values, and elemental and charred organic matter contents.

Depth (cm)	Age (cal y BP)	$\delta D$ (‰)				$\delta^{13}C$ bulk (‰)	%TOC (gC g <sup>-1</sup> )	HI (mg HC g <sup>-1</sup> TOC)	OI (mg O <sub>2</sub> g <sup>-1</sup> TOC)	Total P (mg kg <sup>-1</sup> )	%Char (% area)
		<i>n</i> -C <sub>26</sub>	<i>n</i> -C <sub>28</sub>	<i>n</i> -C <sub>30</sub>	C <sub>3</sub> corr						
1. Mai Maikden (MMII)											
0	100	-127	-132	-114	-139	-20	2.3	140	369	857	7.3
30	112	-157	-131	-133	-172	-18	1.4	100	381	890	28.0
100	4515	-152	-147	-148	-166	-18	1.3	20	358	475	13.3
115	4646	n.a.	n.a.	n.a.	n.a.	-19	0.6	0	1049	150	0.3
130	4777	-163	-140	-139	-176	-19	0.6	0	1025	184	53.2
145	4908	n.a.	n.a.	n.a.	n.a.	n.a.	n.a.	0	1236	147	34.5
170	5126	-133	-162	-156	-144	-20	1.3	49	396	628	10.4
200	5388	-153	-160	-176	-165	-19	0.7	16	893	283	68.5
220	5563	-160	-170	-161	-173	-19	0.9	21	693	253	44.9
250	5825	-136	-143	n.a.	-154	-16	0.6	10	1423	238	0.1
270	6000	-166	-141	-158	-186	-13	1.4	21	378	144	0.0
300	6262	-203	-184	-158	-212	-23	1.3	82	320	112	5.2
320	6437	-204	-197	-174	-213	-22	4.3	81	296	297	21.8
355	6743	-209	-200	-196	-219	-22	5.5	101	321	419	46.3
380	6961	-211	-198	-168	-226	-17	6.0	79	276	376	50.1
400	7096	-198	-194	-189	-207	-22	6.4	48	236	640	55.8
425	7247	-185	-158	-132	-194	-22	0.6	44	432	184	0.3
450	7398	-126	n.a.	-131	-135	-22	0.4	49	479	169	0.0
470	7519	-173	-170	-161	-183	-22	0.7	44	418	182	1.6
500	7626	-190	-194	-183	-203	-19	1.0	30	341	243	7.0
520	7697	-187	-176	-166	-200	-19	1.2	38	299	195	44.1
560	7839	-205	-195	-165	-211	-25	1.0	100	381	93	61.0

580	7910	-163	-176	-164	-172	-22	1.0	112	462	89	0.3
595	7963	-217	-211	-197	-224	-23	5.3	163	297	241	4.6
620	8052	-205	-201	-186	-210	-25	4.5	161	279	139	35.8
640	8123	-178	-174	-171	-191	-18	8.1	112	240	693	68.2

## 2. Adi Kolan (AKIII)

0	0	-127	-131	-121	-145	-15	0.4	58	614	1839	15.4
50	298	-125	-130	-121	-146	-13	1.3	80	468	1872	1.7
100	759	-127	-138	-123	-148	-13	0.7	41	590	1471	0.5
120	1024	-135	-140	-125	-156	-13	0.7	43	541	1799	3.1
130	1157	n.a.	n.a.	n.a.	n.a.	-14	0.7	41	495	1761	0.4
150	1422	-132	-138	-127	-152	-14	0.7	33	619	1466	3.2
170	1687	-123	-135	-124	-143	-13	0.7	30	554	1567	0.4
200	2084	-130	-134	-131	-150	-13	0.5	21	579	1258	1.8
210	2217	-140	-147	-153	-159	-15	0.6	n.a.	n.a.	n.a.	n.a.
220	2349	-126	-129	-125	-145	-14	0.8	15	584	1289	0.6
250	2377	-132	-117	-129	-153	-13	0.8	10	483	1280	14.0
270	2396	-134	-124	-125	-155	-13	0.9	10	361	1251	1.2
300	2424	-131	-122	-113	-151	-13	1.4	7	292	1740	14.8
310	2460	-125	-131	-121	-146	-13	2.2	10	265	1735	33.5
330	2586	-126	-133	-139	-146	-14	2.0	n.a.	n.a.	n.a.	n.a.
350	2711	-129	-123	-115	-150	-13	1.8	3	272	1880	32.6
360	2774	-146	-153	-159	-167	-12	1.8	n.a.	n.a.	n.a.	n.a.
370	2837	-136	-135	-124	-157	-13	1.6	4	286	1712	28.9
400	3025	-138	-148	-137	-159	-12	1.2	4	300	1135	22.8
420	3150	-137	-148	-140	-157	-13	1.3	3	283	1133	50.0
460	3401	-121	-145	-120	-141	-14	0.7	9	363	1235	26.1
480	3527	-110	-127	-112	-128	-15	0.3	0	721	1637	1.4
500	3652	-116	-116	-110	-135	-15	0.2	0	741	1832	3.3

520	3778	-145	-129	-121	-163	-15	0.3	0	330	1611	0.6
540	3903	-145	-135	-124	-164	-15	0.6	9	328	1933	7.9
580	4154	-142	-143	-131	-159	-16	0.1	0	559	1413	0.7
610	4342	-140	-142	-139	-159	-15	0.2	0	476	1976	20.9
620	13742	n.a.	n.a.	n.a.	n.a.	-17	0.1	0	558	1922	16.1
640	13742	-172	-129	-135	-185	-16	0.2	0	436	1964	13.5

### 3. Adigrat (ATI)

0	485	-136	-142	-148	-149	-18	1.5	104	375	974	7.1
30	726	-127	-134	-140	-140	-19	1.2	n.a.	n.a.	n.a.	n.a.
70	1046	-134	-141	-147	-146	-20	0.9	52	464	859	7.6
100	1287	n.a.	n.a.	n.a.	n.a.	-19	0.9	50	475	835	6.4
120	1447	-137	-144	-150	-151	-19	1.0	47	458	824	4.4
150	1688	-144	-150	-157	-157	-19	0.9	49	475	821	5.4
170	1848	-136	-143	-149	-150	-18	0.9	45	464	844	1.0
200	2089	-150	-157	-163	-164	-19	1.1	44	421	991	13.8
230	2225	-133	-139	-145	-148	-17	0.9	n.a.	n.a.	n.a.	n.a.
260	2310	-135	-141	-147	-152	-16	0.4	34	481	935	1.1
300	2422	-135	-142	-148	-151	-17	0.4	32	597	757	0.9
320	2479	-153	-159	-166	-167	-18	0.3	32	731	778	1.0
350	2563	-139	-146	-152	-154	-18	0.4	n.a.	n.a.	n.a.	n.a.
380	2624	-135	-155	-161	-150	-18	0.3	n.a.	n.a.	n.a.	n.a.
430	2707	-149	-142	-148	-162	-19	0.2	14	875	771	1.9
460	2756	-129	-136	-142	-142	-19	0.2	n.a.	n.a.	n.a.	n.a.
500	2823	n.a.	n.a.	n.a.	n.a.	-15	0.1	n.a.	n.a.	1034	7.1
*510	2839	*-59	-66	-72	n.a.	-16	0.1	0	849	n.a.	n.a.
*530	2872	*-107	-114	-120	n.a.	-16	0.0	n.a.	n.a.	n.a.	n.a.

<sup>a</sup>From Gebru et al. (2009) and Terwilliger et al. (2011)

TOC = total organic carbon

$C_3$  corr =  $n$ - $C_{26}$  corrected for D-enrichment from  $C_4$  grasses The oldest of these estimates (ca. 14750 cal y BP) also has +5 ‰ added as a correction for different ice volume (see text).

HI, OI = hydrogen index, oxygen index from Rock-Eval pyrolysis

P = phosphorus

Char = charred organic matter

Table 3. Sequential linear trends in  $\delta D_{n-C26}$  and bulk organic  $\delta^{13}C$  values (Y) with age (X).

Y	Curve type	Breakpt (cal y BP)	Change (from older to younger)			
			All	Oldest to Breakpt	At Breakpt	Breakpt to youngest
1. Mai Maikden (MMII)						
$\delta D_{n-C26}$	5	6035			+	
$\delta^{13}C$ bulk m	5	6035			+	
$\delta^{13}C$ bulk t	6	6115		-	+	+
2. Adi Kolan (AKIII)						
$\delta D_{n-C26}$	1		+			
$\delta^{13}C$ bulk m	5	3435			+	
$\delta^{13}C$ bulk t	6	3435		+	+	-
3. Adigrat (ATI)						
$\delta D_{n-C26}$	6	2440		-	+	+
$\delta^{13}C$ bulk m	5	2110			-	
$\delta^{13}C$ bulk t	6	2680		-	+	-

m = only values corresponding to  $\delta D_{n-C26}$  sample set.

t = all values.

+ =  $\delta$  values increase significantly from older to younger sample ages.

- =  $\delta$  values decrease significantly from older to younger sample ages.

Significance established at  $p \leq 0.05$ .

Curve types for relationship of  $\delta$  (Y) to age (X)

0. no relationship, slope not significantly different from 0.

1. simple linear slope.

2. two sloping lines connected at a breakpt (breakpoint).

3. sloping line from maximum age to a breakpt, followed by no relationship to most recent age.

4. no relationship from maximum age to a breakpt, followed by sloping line to most recent age.

5. two disconnected intervals with slopes not significantly different from 0 but separated at a breakpt (ages older than breakpt  $\neq$  younger ages)

6. two disconnected sloping lines separated at a breakpt.

Table 4. Correlations of soil micromorphological and chemical characteristics to one another and to  $\delta$  values.

	Total P	%Char	%TOC	HI	OI	$\delta D_{n-C26}$
1. MMII						
%Char	n.s.					
%TOC	n.s.	n.s.				
HI	n.s.	n.s.	0.0005			
OI	n.s.	n.s.	-0.0070	-0.0010		
$\delta D_{n-C26}$	n.s.	n.s.	-0.0030	n.s.	0.014	
$\delta^{13}C$ bulk	n.s.	n.s.	n.s.	-0.0070	n.s.	0.040
2. AKIII						
%Char	n.s.					
%TOC	n.s.	0.0040				
HI	n.s.	n.s.	n.s.			
OI	n.s.	-0.0005	-0.0005	n.s.		
$\delta D_{n-C26}$	n.s.	n.s.	n.s.	n.s.	n.s.	
$\delta^{13}C$ bulk	-0.0500	n.s.	0.0005	n.s.	n.s.	n.s.
3. ATI						
%Char	0.0250					
%TOC	n.s.	n.s.				
HI	n.s.	n.s.	0.0005			
OI	n.s.	n.s.	-0.0020	-0.0020		
$\delta D_{n-C26}$	n.s.	n.s.	n.s.	n.s.	n.s.	
$\delta^{13}C$ bulk	n.s.	n.s.	n.s.	n.s.	n.s.	n.s.

Total P = Total Phosphorus (mg P kg<sup>-1</sup> soil)

%Char = charred organic matter (% area)

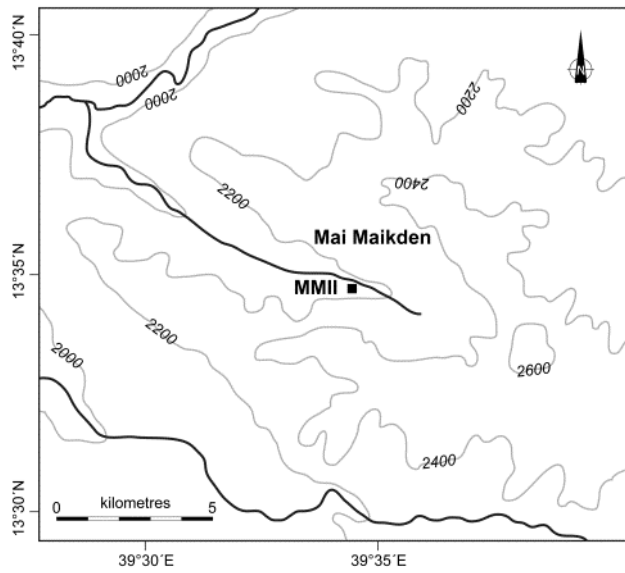
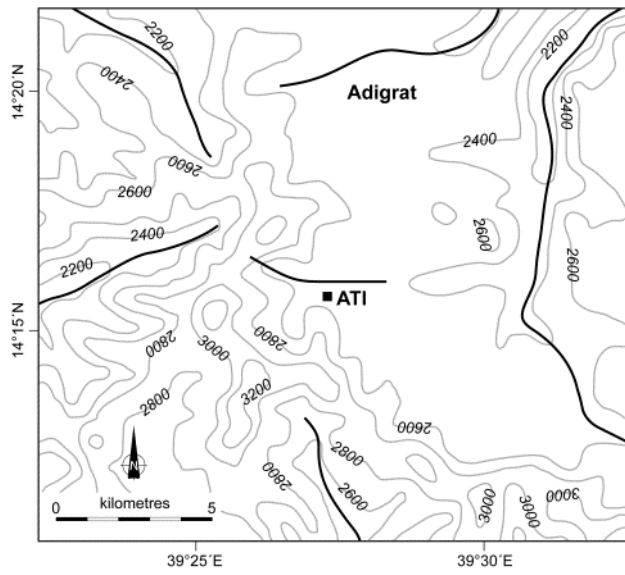
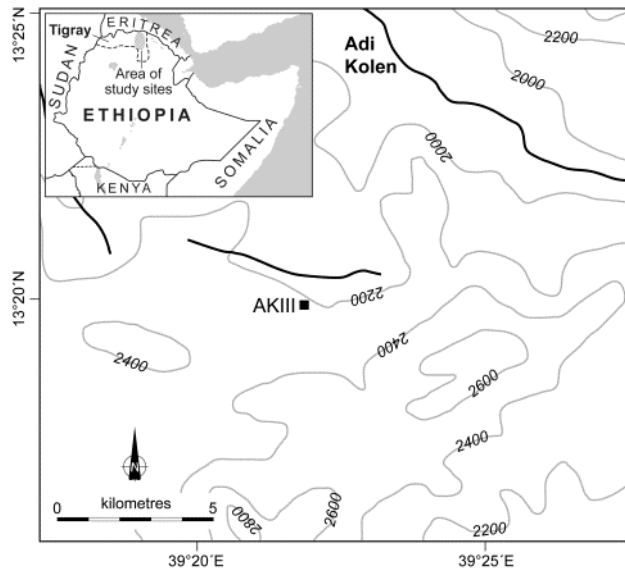
%TOC = % Total organic carbon by weight

HI = Hydrogen Index (mg HC g<sup>-1</sup> TOC)

OI = Oxygen Index mg O<sub>2</sub> g<sup>-1</sup> TOC

numbers = maximum *p* values of significant correlations where negative values denote negative correlations

n.s. = not significant (*p* > 0.05)



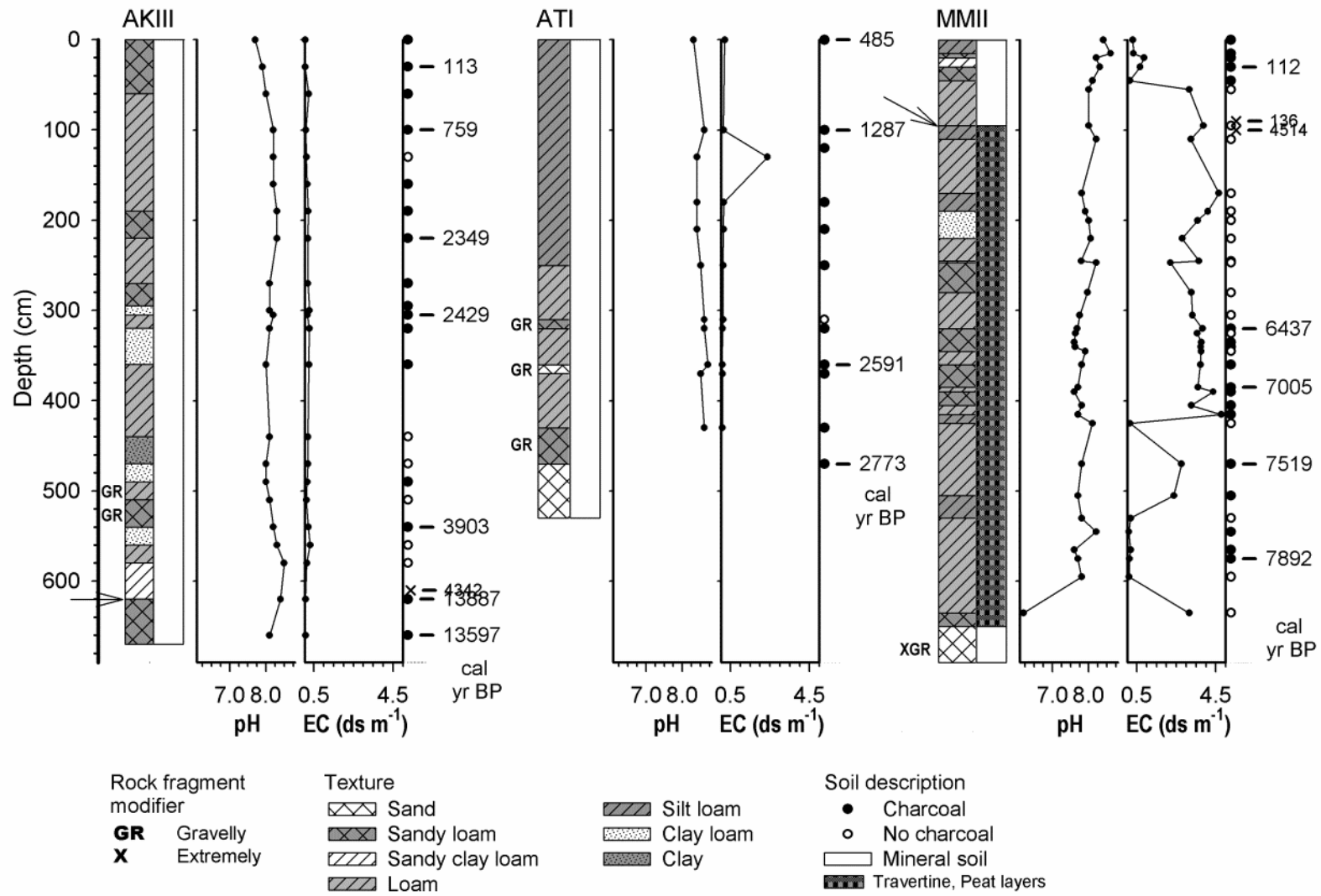


Fig. 2



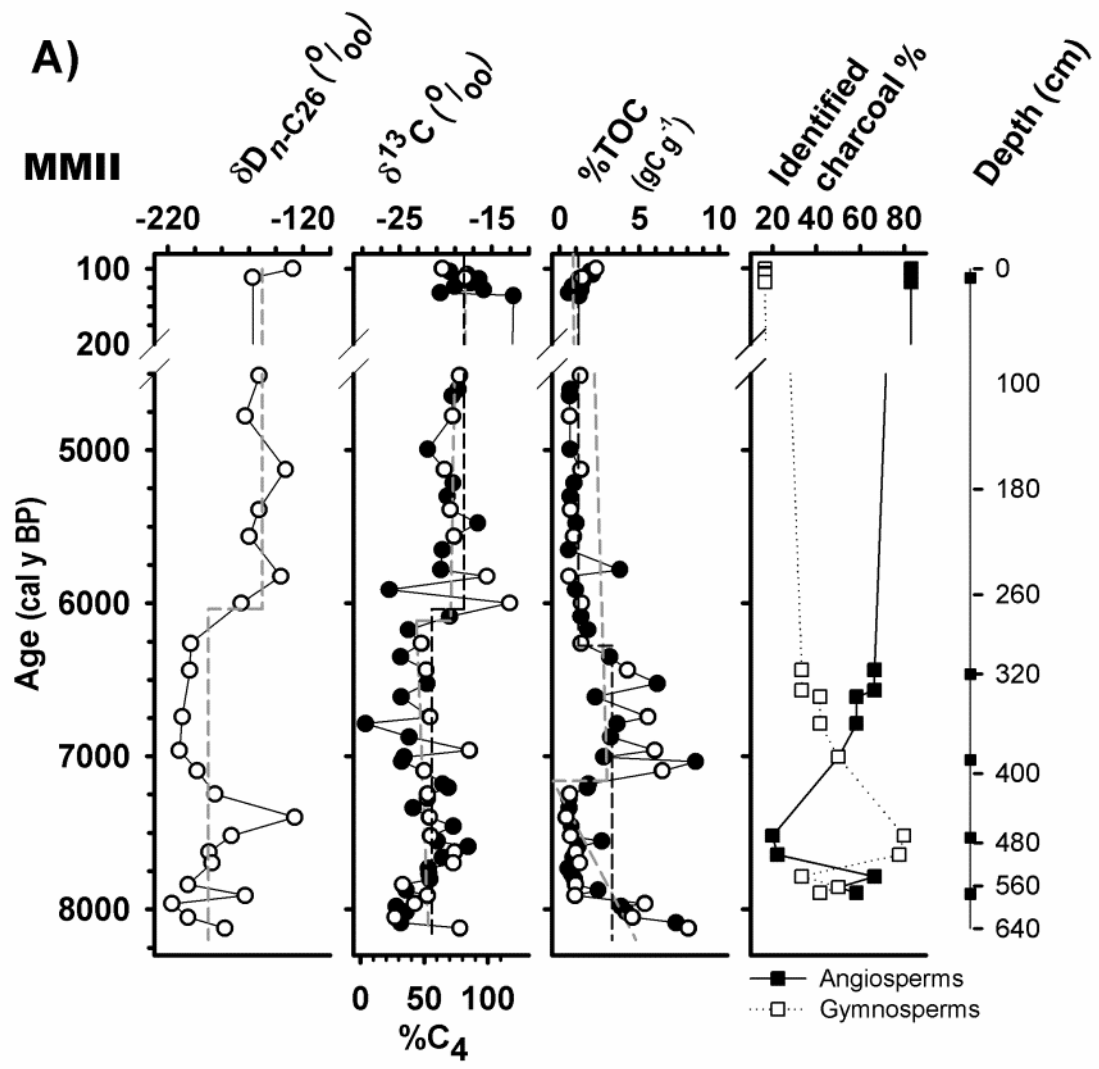


Fig. 4A

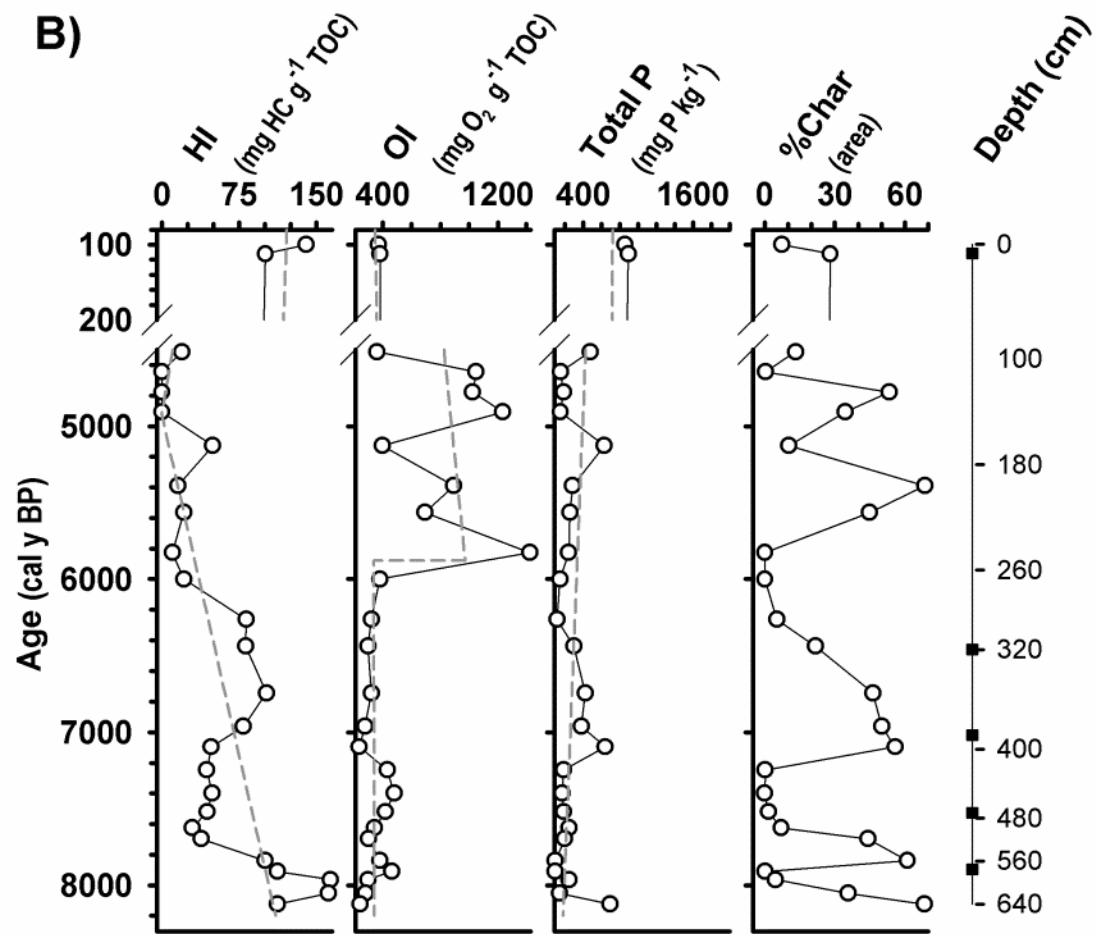


Fig. 4B

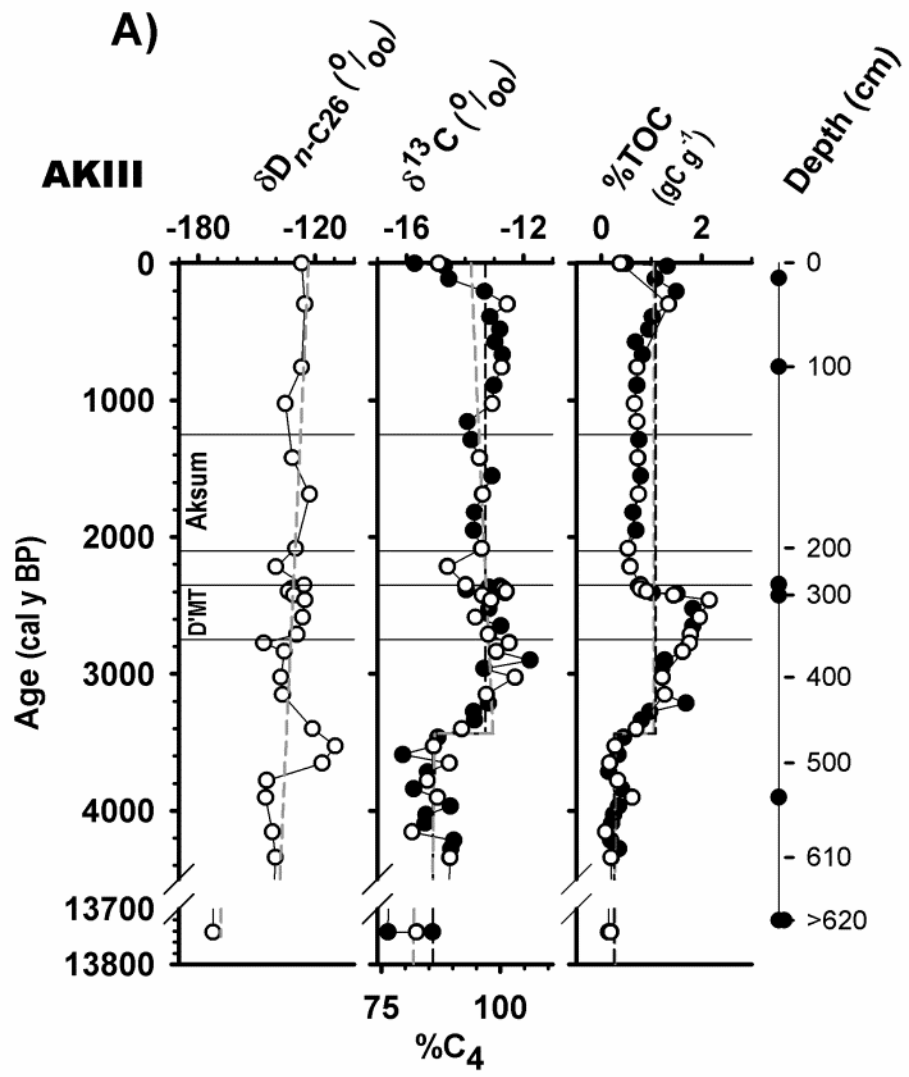


Fig. 5A

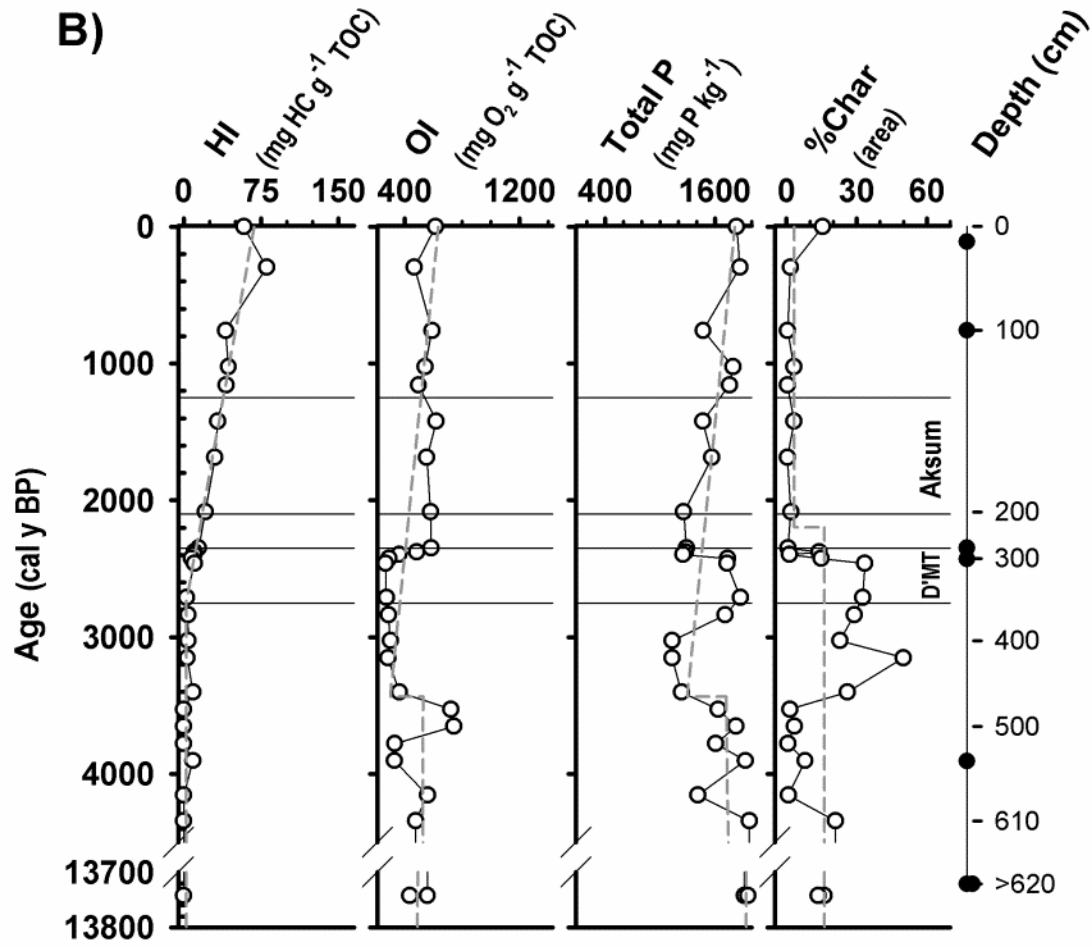


Fig. 5B

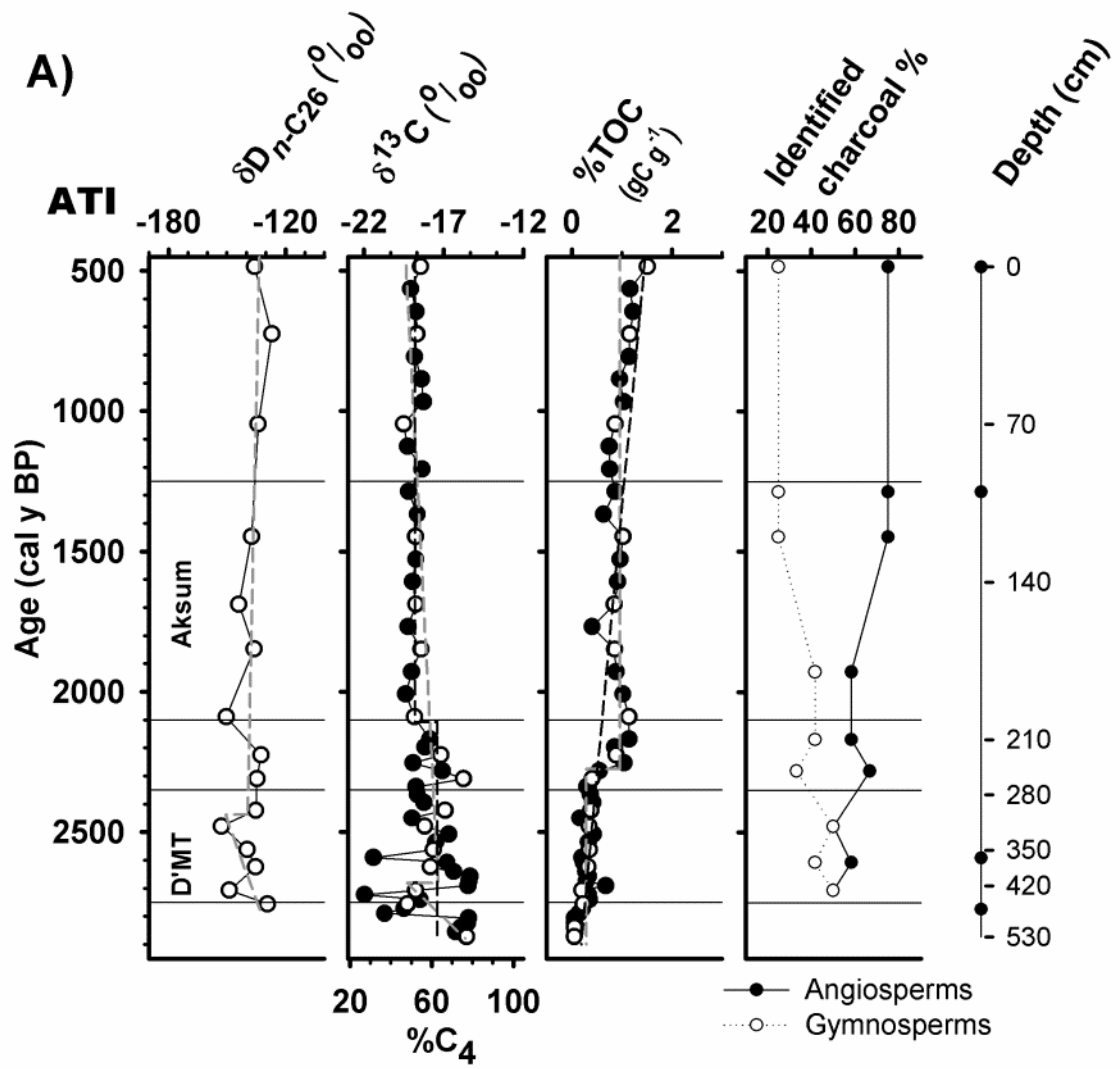


Fig.6A

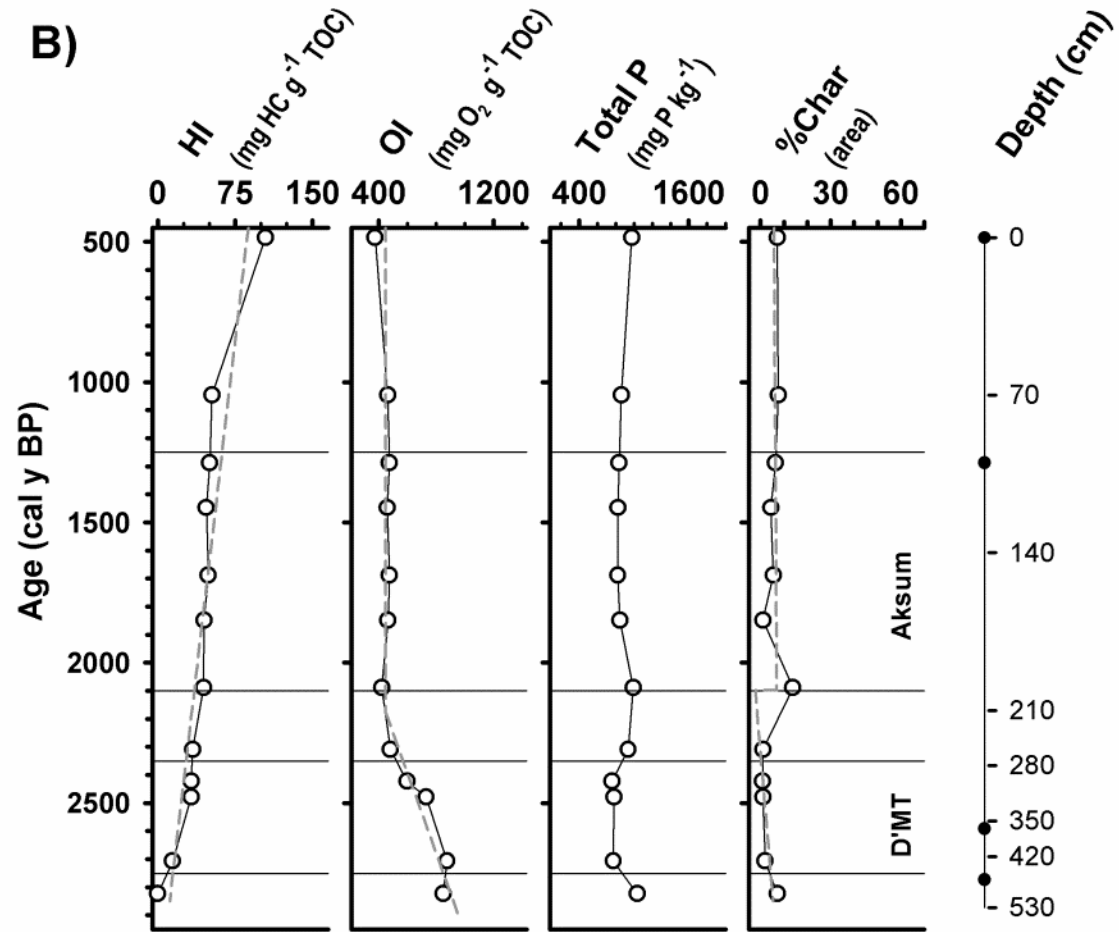


Fig. 6B